THE UNIVERSITY OF MICHIGAN
RADIO ASTRONOMY OBSERVATORY

Report 67-7

MOTION AND STABILITY

OF A SPINNING CABLE-CONNECTED SYSTEM IN ORBIT

S. A. Crist

DEPARTMENT OF ASTRONOMY
DEPARTMENT OF ELECTRICAL ENGINEERING

THE UNIVERSITY OF MICHIGAN

RADIO ASTRONOMY OBSERVATORY

Report 67-7

MOTION AND STABILITY OF A SPINNING CABLE-CONNECTED SYSTEM IN ORBIT

S. A. Crist

Sponsored by National Aeronautics and Space Administration

Grant NGR-23-005-131

June 1967
(Revised December 1967)

Department of Astronomy

TABLE OF CONTENTS

LIST OF ILLUSTRATIONS

LIST OF SYMBOLS

Given below is the most common use of each symbol. In some places a symbol will be defined differently, but its meaning in each context is defined at that point in the text.

A	Wire cross-sectional area
C_i	Damping coefficient for given spring
e_i	Stretched length of a given spring
E	Young's modulus of elasticity
G	Product of universal gravitational constant and mass of the Earth
k, k_i	Spring constant for a given spring
ℓ, ℓ_i	Coordinate to a given mass
ℓ_{i0}	Unstretched length of a given spring
L, L_s, L_M	Various Lagrangian functions
M_i	Mass of a given point
Q_i	Generalized force
q_i	Deviation from a given nominal motion
R	Radius from center of rotation of orbiting body to Earth's center of mass
$\bar{r}$, r	Radius vector or radius
T_s, T_M	Kinetic energy function
T	Tension in wire
t	time
u	Transverse displacement of continuous wire

v	Axial displacement of continuous wire
V_E, V_G	Potential functions
W_O	Angular momentum
β	Rotational frequency
ϵ	Axial strain
θ	Orbital position measured counter-clockwise from perigee
λ_i	Given eigenvalue of a matrix
ρ	Mass/unit length of wire
τ	Period of cyclic motion
φ_i	Angular position of a given mass point in the orbiting body
ψ_i	Angular position of a given mass point out of the orbital plane
ω	Frequency of rotation or vibration
$(^{\cdot})$	Denotes differentiation with respect to time
$(\ )_{u,v,r}$	Denotes partial differentiation with respect to u,v,r.

Matrices

$[A]$	Square matrix of coefficients for a linear system of differential equations
$\{b(t)\}$	Column matrix of forcing functions
$[F(t)]$ or $[F'(t)]$	Fundamental matrix of linear system of differential equations
$[I]$	Identity matrix
$[J]$	Jordan normal form of monodromy matrix
$[M]$	Monodromy matrix from Floquet theory
$\{q\}$ and $\{\dot{q}\}$	Column matrices of dependent variables and associated time derivatives

CHAPTER I

INTRODUCTION

The dynamics of nonrigid satellites has been the subject of interest for some time. There are numerous references in the literature which refer to problems that have been solved either by theoretical analysis or by emperical methods. For example, many satellites are now stabilized by using the gradient of the Earth's gravitational field.

The gravitational force which the Earth exerts on a second body decreases as the inverse of the square of the distance between the two mass centers. It has been shown that if a nonsymmetric satellite with damping is placed in circular or nearly circular orbit around a much larger body, the satellite will become stabilized about an inertia axis which always points along the local vertical. This orientation allows a satellite antenna to maintain, at all times, some desired pointing position relative to the Earth.

An analysis of this problem for a dumbbell shaped satellite which is extensible but may not deform in bending appears in an article by Paul[1]. In this case, the system always stabilizes itself about a fixed direction relative to the Earth. This is not always desirable as in the case of a manned space capsule spinning about its booster vehicle at the end of a cable to provide artificial gravity for the astronaut. Here it is desirable for the spinning to continue indefinitly without the addition of thrust.

The problem of a cable connected system spinning is orbit raises two basic stability questions: (1) will the system continue to move at a fairly constant spin rate in the predicted orbit and (2), will the internal motion of the system, in this case the connecting cable, remain bounded near some desired motion? Several papers on these two problems have been written. All deal only with motion in the plane of the orbit.

In connection with the first stability question, the paper by Pittman and Hall[2] claims that any such system is inherently stable since it is moving in a conservative force field. This is true, but they do not make statements about the limits of these bounds and, as will be shown later, the limits may be undesirable from a practical point of view. The study by Austin[3] does not consider the gravity effects but restricts itself to an investigation of nonlinear effects due to rotation. His model is also the extensible dumbbell for which he concludes that nonlinearities due to rotational effects become important only when the spin rate is high. He does not consider the dynamics of the connecting cable.

Thus, in answer to the first stability question, it would seem that there is nothing to insure that the system will not leave its predicted Keplerian orbit and approach the Earth's surface at a higher and higher spin rate so that the total energy is conserved.

The second question, that of cable dynamics, has been studied by several authors. The papers by Chobotov[4], Pengelly[5], Tai and Loh[6], and Targoff[7] all treat the problem of a cable connected system spinning in orbit. Each assumes the cable to have negligible bending stiffness, and to be of a uniform, linear elastic material. The bodies which the

cable connects are assumed to be point masses by all authors. However, Pengelly also deals with finite rigid bodies. The paper by Targoff carries the analysis of cable dynamics the furthest so the present discussion will be restricted to his paper.

Targoff derives the equations of motion by summing forces on each mass element of the system and satisfying static equilibrium with the corresponding D'Alembert forces. An assumption of small deflections is made from the start of the analysis. Coriolis effects are also neglected to uncouple the equations which he derives. The first assumption, that of small deflections, is commonly made when studying dynamic systems, and can usually be justified if stability is demonstrated. However, it is not clear that the second assumption, that of neglecting the Coriolis effects, can be justified. Even in the case of slowly spinning systems, the forces retained in the analysis also tend to decrease with the spin rate as do the Coriolis forces. Unfortunately, the equations derived for the spinning cable system are too complex to lend themselves to analytical solution if the Coriolis effects are retained.

A survey paper by Ashley[8] points out that, in general, a systematic approach to the problem of gravity gradient excited spinning systems needs to be considered. The authors mentioned above have, each in his own way, attacked some aspect of the problem by various techniques. Their methods of analysis soon reach the limit of their applicability when applied to relatively simple systems. This is not to say that the results obtained from these studies are not valid or useful. The results of a simplified analytic approach are many times instructive and serve as a starting point of a more general analysis.

The purpose of the present study is to present a more general approach. The methods of analysis described here can be applied to general cable connected structures. The method presented is specifically applied to the problem of a point mass spinning about a much heavier body to which it is connected by a linear elastic, constant density, constant cross sectional area cable. The system, in turn, is in an orbit about a third body as can be seen in Figure 1. This particular configuration is a special case of the more general model considered by Targoff[7] and others[4,5,6].

For the more general model, the center of mass is not necessarily attached to a physical point on the system. In the case considered here, the center of mass is assumed to be at the center of the heavier of the two orbiting masses. This assumption is reasonable for a system which has a heavy body at the center of the structure. If the more general configuration were to be studied in the same way as that proposed here, as a rule, two constraint equations would have to be imposed which would specify the origin of the coordinate system of the orbiting bodies as the center of mass of the orbiting system.

There are, in fact, two cases where it is not necessary to include the constraint equations: (1) the case mentioned above in which the center of mass is assumed to be at the center of the heavier body and (2) the dumbbell case, also mentioned previously. In the case of the latter, the center of mass is on a line between the two end mass points if the connecting cable is assumed to be massless. Both cases are considered in the work.

In the first part of this study, the equations of motion are

derived by applying Hamilton's principle to the action integral for the cable connected system shown in Figure 1. The equations derived are nonlinear, coupled, partial differential equations with time dependent boundary conditions. Three special cases are shown to come from the general equations when appropriate assumptions are imposed. The complexity of the general nonlinear equations and the corresponding linearized equations seems to preclude analytical solution unless some rather severe assumptions are made. Thus, even though a systematic approach to the problem via Hamilton's principle produces the exact equations of motion for the system, little information concerning stability or motion can be obtained without limiting assumptions.

Because of the difficulties encountered above, it is proposed in chapter III that the cable be approximated by linear elastic, massless springs. The Lagrange equations of motion for the lumped system are shown to be a system of nonlinear, ordinary differential equations. Damping is included in the equations and its effects of stability investigated. Previous authors have given only a brief and, perhaps, oversimplified look at damping effects.

The simplest lumped mass model, the dumbbell, is then used to examine, in more detail, the bounds on the types of motion which can occur within the energy levels of the conservative system. The orbits in which the dumbbell may move are shown to be essentially those in which a point mass may move; however, a small change in orbit of the dumbbell means a sizable change in spin rate.

The bounds are found by examining the ficticious potential function for the dumbbell system. Results from a numerical integration of the

exact equations for the dumbbell indicate that, for most cases, it is reasonable to assume that the center of mass of the system moves in a Keplerian orbit. This affords one the luxury of being able to calculate the position of the center of mass independent of the relative motion of the system. It is shown that the motion of a dumbbell whose center of mass moves in an undisturbed Keplerian orbit, and that of a light mass spinning about a very heavy mass which also moves in an undisturbed Keplerian orbit are almost identical. The latter model is henceforth refered to as the single mass model since only the lighter mass moves relative to the orbital point. The above result is used to justify the original model and orbital assumption considered.

Next, the results of an analysis of gravity gradient stabilization of the single mass model, which is equivalent to the dumbbell, are shown to agree with the work of Paul[1] and also with the conclusions reached from examination of the ficticious potential function.

The analysis then proceeds to the case where the single mass is spinning in orbit. The linearized equations are shown to be forced, ordinary differential equations with periodic coefficients. A method given in the book by Cesari[9] allows one to study the stability of the system of linear equations with periodic coefficients. The method, due to Floquet, may be applied through numerical integration to any set of linear ordinary differential equations having periodic coefficients. The importance of this result is that any general configuration can be systematically analysed by lumping the distributed mass of the cables, linearizing the equations, and applying Floquet theory by numerical integration.

The investigation then turns to the dynamics of the connecting cable. A justification of the lumped analysis is shown by comparing natural frequencies obtained from both a distributed mass and a lumped mass analysis of the nonspinning cable. The effects of damping in the lumped model are considered and shown to be ineffective in damping out transverse motions.

A brief analysis is given to justify neglecting out-of-plane motions of the connecting cable in any analysis of in-plane motions.

The final section gives an example of how finite bodies may be incorporated into the lumped model to determine the modes of stability and motion for a cable connected system where the rigid body motion of the connected bodies may be important.

The impetus for this work arose from a NASA grant to the Radio Astronomy Observatory of the University of Michigan to study the feasibility of a very large cable connected orbiting and spinning antenna for radio astronomy observation near the 1Mc. frequencies (see reference 10 for more details of the antenna). The single mass model considered in this study is, in fact, an approximation to a portion of that structure. The general approach to the problem was devised to allow analysis of the complete structure in orbit.

CHAPTER II

DISTRIBUTED MASS SYSTEM

The system to be considered consists of a point mass subsatellite connected to a much heavier point mass which moves in an undisturbed Keplerian orbit around the Earth, as shown in Figure 1. It is assumed that the motions of the subsatellite do not disturb the heavier mass. The assumption of a point mass subsatellite is a simplifying assumption which can easily be dropped, if the rigid body motions are to be considered, as will be shown in chapter V. The cable is assumed to have constant linear elastic properties, constant mass distribution and a constant cross sectional area. These three assumptions are not necessary for the analysis, but do simplify the work required and are reasonable for most applications. The motions are restricted to the orbital plane since all the features of the analysis can be shown for this type of motion. A further justification of this restriction is presented in chapter IV where the cable is free to move out of the plane. The motion reference line shown in Figure 1 and given by the coordinate φ is general and may be specified as the rigid body motion of the cable-subsatellite system. The definition of φ is changed to suit the particular case studied.

The radial and tangential deflections of the cable, $v(r,t)$ and $u(r,t)$ respectively, are measured from the undeflected, rigid body reference line given by r and φ. Hence, the system is considered to be rotating if $\dot{\varphi} \neq 0$.

Using this model and the above assumptions, the exact equations of motion are derived via Hamilton's principle. They are linearized and solved for three special cases of constant tension: (1) nonrotating, where $\dot{\varphi} = 0$, with no gravity gradient effects, (2) rotating, where $\dot{\varphi}$ = constant, again with no gravity gradient effects, and (3) rotating in the gravity gradient with $\dot{\varphi}$ = a function of time. These three cases are shown to agree with previous work and they also demonstrate the assumptions which must be made to obtain solutions for the distributed mass analysis.

We now proceed to derive the equations of motion. The radius vector from the Earth's center to any mass point, dm, is given by

$$\bar{r} = [R\cos\theta + (r+v)\cos\varphi - u\sin\varphi]\bar{i} + [R\sin\theta + (r+v)\sin\varphi + u\cos\varphi]\bar{j} \tag{1}$$

The square of the magnitude of the velocity vector is given by

$$\begin{aligned}|\dot{\bar{r}}|^2 = {} & \dot{R}^2 + (R\dot{\theta})^2 + \dot{v}^2 + \dot{u}^2 + [(r+v)^2 + u^2]\dot{\varphi}^2 - 2\dot{u}\dot{v}\dot{\varphi} + 2\dot{u}(r+v)\dot{\varphi} \\ & + 2\cos(\varphi-\theta)[\ddot{R}v + R\ddot{\theta}u + R\dot{\theta}(r+v)\dot{\varphi} - \dot{R}u\dot{\varphi}] \\ & + 2\sin(\varphi-\theta)[-\ddot{R}u - \dot{R}(r+v)\dot{\varphi} + R\ddot{\theta}v - R\dot{\theta}u\dot{\varphi}].\end{aligned} \tag{2}$$

The Lagrangian consists of the following terms

$$L_s = T_s - V_E - V_G$$

where $T_s \equiv$ Kinetic energy of cable

$V_E \equiv$ the elastic potential of the cable

and $V_G \equiv$ the potential due to the gravity field.

The term, T_s, is given by

$$(3)\quad T_s = 1/2\int_0^{\ell} \rho \left|\dot{\vec{r}}\right|^2 dr = 1/2\,\rho \int_0^{\ell} \left|\dot{\vec{r}}\right|^2 dr \qquad \text{for } \rho = \text{const.}$$

where ℓ = length of unstretched cable and ρ = mass/unit length. The elastic potential, V_E, is given by

$$V_E = 1/2\int_0^{\ell} AE\,\epsilon^2 dr$$

where ϵ is the axial strain of the cable, A is its crossectional area and E is Young's modulus. This definition of strain energy assumes only axial strains and neglects bending strains. This assumption is valid for a long thin cable, even when transverse deflections are allowed, if the local radius of curvature remains large. The axial strain is given by

$$\epsilon \equiv \lim_{\Delta r \to 0} \left(\frac{\Delta s - \Delta r}{\Delta r} \right).$$

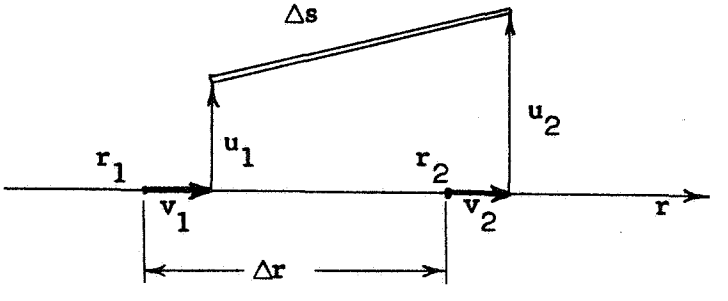

For $$\Delta s = \sqrt{[\Delta r + (v_2 - v_1)]^2 + (u_2 - u_1)^2}\ ,$$

we get

$$\lim_{\Delta r \to 0} \left(\frac{\sqrt{[\Delta r + (v_2 - v_1)]^2 + (u_2 - u_1)^2} - \Delta r}{\Delta r} \right) = \sqrt{1 + 2v_r + v_r^2 + u_r^2} - 1$$

where v_r implies $\frac{\partial v}{\partial r}$ and u_r implies $\frac{\partial u}{\partial r}$.

For small displacements, this reduces to the familiar one-dimensional strain displacement relation

$$\epsilon = v_r \ .$$

Finally, for V_E,

$$(4) \qquad V_E = \frac{AE}{2} \int_0^{\ell} \left[\sqrt{1 + 2v_r + v_r^2 + u_r^2} - 1 \right]^2 dr \ .$$

The potential V_G, is given by

$$V_G = - \int_0^{\ell} \frac{G \rho}{|\bar{r}|} \, dr$$

where G = product of Universal gravity constant and mass of Earth.

After substitution for $|\bar{r}|$,

$$(5) \quad V_G = - G\rho \int_0^{\ell} \frac{dr}{\sqrt{R^2 + (r + v)^2 + u^2 + 2R[(r + v)\cos(\varphi - \theta) - u \sin(\varphi - \theta)]}} \ .$$

Hence, L_s, is expressed by equations (3), (4), and (5). The Lagrangian for the end mass contribution, L_M, is found by replacing the integral of ρdr by M and evaluating the functions at $r = \ell$ in expressions (3) and (5), i.e.

$$(6) \qquad T_M = 1/2 \ M |\dot{\bar{r}}|^2 \Big|_{r = \ell} \ .$$

The action integral is defined as

$$(7) \qquad J(v,u) = \int_{t_1}^{t_2} L dt$$

where $L = L_s + L_M$.

Expressing the varied functions as

$$v^*(r,t) = v(r,t) + \epsilon v_1(r,t)$$

and

$$u^*(r,t) = u(r,t) + \epsilon u_1(r,t)$$

we may compute the first variation of the action integral. According to Hamilton's principle, the first variation must be stationary.

Hence for

$$J = \int_{t_1}^{t_2} \int_0^{\ell} L_s \, dr dt + \int_{t_1}^{t_2} L_M \, dt$$

we get the variation (see reference 11)

$$(8) \quad \delta J = \epsilon \int_{t_1}^{t_2} \int_0^{\ell} \left(L_{s_v} - \frac{\partial L_{s_{v_r}}}{\partial r} - \frac{\partial L_{s_{\dot{v}}}}{\partial t} \right) v_1(r,t) \, dr dt$$

$$+ \epsilon \int_{t_1}^{t_2} \int_0^{\ell} \left(L_{s_u} - \frac{\partial L_{s_{u_r}}}{\partial r} - \frac{\partial L_{s_{\dot{u}}}}{\partial t} \right) u_1(r,t) \, dr dt$$

$$+ \epsilon \int_{t_1}^{t_2} \int_0^{\ell} \left[\frac{\partial}{\partial t} \left(L_{s_{\dot{v}}} v_1 + L_{s_{\dot{u}}} u_1 \right) + \frac{\partial}{\partial r} \left(L_{s_{v_r}} v_1 + L_{s_{u_r}} u_1 \right) \right] dr dt$$

$$+ \epsilon \int_{t_1}^{t_2} \left(L_{M_v} - \frac{\partial}{\partial t} L_{M_{\dot{v}}} \right) v_1(\ell,t) \, dt + \epsilon \int_{t_1}^{t_2} \frac{\partial}{\partial t} \left(L_{M_{\dot{v}}} v_1(\ell,t) \right) dt$$

$$+ \epsilon \int_{t_1}^{t_2} \left(L_{M_u} - \frac{\partial}{\partial t} L_{M_u^{\cdot}} \right) u_1(\ell,t)dt + \epsilon \int_{t_1}^{t_2} \frac{\partial}{\partial t} \left(L_{M_u^{\cdot}} u_1(\ell,t) \right) dt$$

where L_{s_v} implies $\frac{\partial L_s}{\partial v}$. The varied functions must vanish at the end of the time interval, hence

$$u_1(r,t)\Big|_{t_1,t_2} = v_1(r,t)\Big|_{t_1,t_2} \equiv 0.$$

The geometric boundary conditions are $v(0,t) = u(0,t) = 0$. Applying these conditions to equation (8) reduces it to

$$(9) \quad \delta J = \epsilon \int_{t_1}^{t_2} \int_0^{\ell} \left(L_{s_v} - \frac{\partial}{\partial r} L_{s_{v_r}} - \frac{\partial}{\partial t} L_{s_v^{\cdot}} \right) v_1(r,t)drdt$$

$$+ \epsilon \int_{t_1}^{t_2} \int_0^{\ell} \left(L_{s_u} - \frac{\partial}{\partial r} L_{s_{u_r}} - \frac{\partial}{\partial t} L_{s_u^{\cdot}} \right) u_1(r,t)drdt$$

$$+ \epsilon \int_{t_1}^{t_2} \left(L_{s_{v_r}} v_1 + L_{s_{u_r}} u_1 \right) \Big|_{r=\ell} dt$$

$$+ \epsilon \int_{t_1}^{t_2} \left(L_{M_v} - \frac{\partial}{\partial t} L_{M_v^{\cdot}} \right) v_1(\ell,t)dt$$

$$+ \epsilon \int_{t_1}^{t_2} \left(L_{M_u} - \frac{\partial}{\partial t} L_{M_u^{\cdot}} \right) u_1(\ell,t)dt \quad .$$

For the variation to vanish, each of the first two integrals must vanish. Thus, we obtain the equations of motion from the first two integrals, namely

$$(10) \qquad L_{s_v} - \frac{\partial}{\partial r} L_{s_{v_r}} - \frac{\partial}{\partial t} L_{s_{\dot{v}}} = 0$$

and

$$(11) \qquad L_{s_u} - \frac{\partial}{\partial r} L_{s_{u_r}} - \frac{\partial}{\partial t} L_{s_{\dot{u}}} = 0 \ .$$

After collecting the integrals having u_1 and v_1 respectively, we obtain the following natural boundary conditions for the free end of the cable,

$$(12) \qquad L_{s_{u_r}}\Big|_{r = \ell} + L_{M_u} - \frac{\partial}{\partial t} L_{M_{\dot{u}}} = 0$$

$$(13) \qquad L_{s_{v_r}}\Big|_{r = \ell} + L_{M_v} - \frac{\partial}{\partial t} L_{M_{\dot{v}}} = 0 \ .$$

The equations and boundary conditions at this point are in terms of the two contributions to the Lagrangian. To compute the equations in terms of our displacement functions, u and v, the following derivatives are calculated

$$(14) \quad L_{s_v} = \rho \left\{(r+v)\dot{\varphi}^2 + R\ddot{\theta}\dot{\varphi} \cos(\varphi - \theta) - R\ddot{\varphi} \sin(\varphi - \theta) + \ddot{u}\varphi \right\}$$

$$- \frac{G \rho [(r + v) + R \cos(\varphi - \theta)]}{\left\{R^2 + (r + v)^2 + u^2 + 2R[(r + v) \cos(\varphi - \theta) - u \sin(\varphi - \theta)]\right\}^{3/2}}$$

$$(15) \quad L_{s_u} = \rho \left\{u\dot{\varphi}^2 - R\ddot{\theta}\varphi \sin(\varphi - \theta) - \ddot{v}\varphi - R\ddot{\varphi} \cos(\varphi - \theta)\right\}$$

$$- \frac{G \rho [u - R \sin(\varphi - \theta)]}{\left\{R^2 + (r + v)^2 + u^2 + 2R[(r + v) \cos(\varphi - \theta) - u \sin(\varphi - \theta)]\right\}^{3/2}}$$

$$(16)\qquad -\frac{\partial L_{s_{v_r}}}{\partial r} = AE\left\{v_{rr}\left[1 - \frac{1}{\sqrt{1 + 2v_r + v_r^2 + u_r^2}}\right] + \frac{(1 + v_r)(v_{rr} + v_r v_{rr} + u_r u_{rr})}{(1 + 2v_r + v_r^2 + u_r^2)^{3/2}}\right\}$$

$$(17)\qquad -\frac{\partial L_{s_{u_r}}}{\partial r} = AE\left\{u_{rr}\left[1 - \frac{1}{\sqrt{1 + 2v_r + v_r^2 + u_r^2}}\right] + \frac{u_r(v_{rr} + v_r v_{rr} + u_r u_{rr})}{(1 + 2v_r + v_r^2 + u_r^2)^{3/2}}\right\}$$

$$(18)\qquad -\frac{\partial L_{s_v}}{\partial t} = -\rho\left\{\ddot{v} + [\ddot{R} + R\dot{\theta}(\dot{\varphi} - \dot{\theta})]\cos(\varphi - \theta) + [-\dot{R}(\dot{\varphi} - \dot{\theta}) + \ddot{R}\theta + R\ddot{\theta}]\sin(\varphi - \theta) - \ddot{u}\varphi - u\ddot{\varphi}\right\}$$

$$(19)\qquad -\frac{\partial L_{s_u}}{\partial t} = -\rho\left\{\ddot{u} + \ddot{v}\varphi + (r + v)\ddot{\varphi} + [\ddot{R}\theta + R\ddot{\theta} - \dot{R}(\dot{\varphi} - \dot{\theta})]\cos(\varphi - \theta) + [-R\dot{\theta}(\dot{\varphi} - \dot{\theta}) - \ddot{R}]\sin(\varphi - \theta)\right\}.$$

The terms in equations (14) and (15) which came from the gravity potential may be expanded in terms of the ratio of the body dimensions to the orbital radius. This expansion converges quite rapidly since $R \ggg r, v, u$. Keeping up to first order terms, we get for these terms respectively

$$(20)\quad -\frac{G\rho}{R^2}\cos(\varphi-\theta)-\frac{G\rho}{R^3}(r+v)+\frac{3G\rho}{R^3}\left[(r+v)\cos^2(\varphi-\theta)-\frac{u\sin 2(\varphi-\theta)}{2}\right]$$

and

$$(21)\quad -\frac{G\rho}{R^2}\sin(\varphi-\theta)-\frac{G\rho}{R^3}u-\frac{3G\rho}{R^3}\left[\{(r+v)\sin 2(\varphi-\theta)\}/2-u\sin^2(\varphi-\theta)\right].$$

It can be noted here that if all the terms multiplied by $\sin(\varphi-\theta)$ and $\cos(\varphi-\theta)$ are collected, their coefficients from equations (14) and (15) are

$$(22)\quad \rho\left(\ddot{R}-R\dot{\theta}^2+\frac{G}{R^2}\right)\quad\text{and}\quad\rho\left(R\ddot{\theta}+2\dot{R}\dot{\theta}\right).$$

These two coefficients are zero if we let R and θ be governed by Keplerian equations of motion which was assumed at the beginning of the problem.

Finally, the nonlinear, partial differential equations for plane motion for the linear elastic subsatellite-cable system after expanding the gravity potential contribution are

$$(23)\quad \ddot{v}=(r+v)\left\{\dot{\varphi}^2+\frac{G}{2R^3}\left[1+3\cos 2(\varphi-\theta)\right]\right\}+u\left\{\ddot{\varphi}-\frac{3G}{2R^3}\sin 2(\varphi-\theta)\right\}$$

$$+ 2\dot{u}\dot{\varphi} + \frac{AE}{\rho}\left\{v_{rr}\left[1 - \frac{1}{\sqrt{1 + 2v_r + v_r^2 + u_r^2}}\right]\right.$$

$$\left. + \frac{(1 + v_r)(v_{rr} + v_r v_{rr} + u_r u_{rr})}{(1 + 2v_r + v_r^2 + u_r^2)^{3/2}}\right\}$$

and

$$(24)\quad \ddot{u} = u\left\{\dot{\varphi}^2 + \frac{G}{2R^3}[1 - 3\cos 2(\varphi - \theta)]\right\}$$

$$- (r + v)\left\{\ddot{\varphi} - \frac{3G}{2R^3}\sin 2(\varphi - \theta)\right\} - 2\dot{v}\dot{\varphi}$$

$$+ \frac{AE}{\rho}\left\{u_{rr}\left[1 - \frac{1}{\sqrt{1 + 2v_r + v_r^2 + u_r^2}}\right] + \frac{u_r(v_{rr} + v_r v_{rr} + u_r u_{rr})}{(1 + 2v_r + v_r^2 + u_r^2)^{3/2}}\right\}.$$

Upon identifying the coefficients as the point mass in orbit equations of motion, the boundary conditions become

$$(25)\quad \ddot{v} = (r + v)\left\{\dot{\varphi}^2 + \frac{G}{2R^3}[1 + 3\cos 2(\varphi - \theta)]\right\}$$

$$+ u\left\{\ddot{\varphi} - \frac{3G}{2R^3}\sin 2(\varphi - \theta)\right\} + 2\dot{u}\dot{\varphi} \quad \triangleq$$

$$- \frac{AE}{M}\left\{1 - \frac{1}{\sqrt{1 + 2v_r + v_r^2 + u_r^2}}\right\}(1 + v_r) \quad @\ r = l$$

and

$$(26)\quad \ddot{u} = u\left\{\dot{\varphi}^2 + \frac{G}{2R^3}\left[1 - 3\cos 2(\varphi - \theta)\right]\right\}$$

$$- (r + v)\left[\ddot{\varphi} - \frac{3G}{R^3}\sin 2(\varphi - \theta)\right] - 2\dot{v}\dot{\varphi}$$

$$- \frac{AE}{M}\left[1 - \frac{1}{\sqrt{1 + 2v_r + v_r^2 + u_r^2}}\right] u_r \quad @\, r = \ell$$

The equations of motion are a function of two variables, time and distance. They are forced through the gyroscopic and gravity gradient terms and coupled through the gyroscopic, the elastic, and the gravity gradient terms. The boundary conditions for the free end exibit the same form as the equations of motion and are time dependent. An analytic solution of this set of equations is hopeless. However, there are certain interesting and informative special cases that may be studied if appropriate simplifying assumptions are made.

1. Case I - Non-spinning in Free Space

If we do the following: (1) let $R = \infty$ so that the gravity effects vanish, (2) let $\dot{\varphi} = 0$, which implies that the system is non-rotating and, finally, (3) prescribe the tension by setting $AEv_r = T = \text{constant}$, we have the case corresponding to that of a cable vibrating with a constant tension between fixed walls. If the above restrictions are placed on equation (24) and it is then linearized, we get the familiar vibrating string equation

(27) $$\ddot{u} = \frac{T}{\rho} u_{rr}$$

with boundary conditions $u(0,t) = u(\ell,t) = 0$. The natural frequencies are easily found to be

$$\omega_n = \frac{n\pi}{\ell}\sqrt{\frac{T}{\rho}} \qquad n = 1, 2, 3, \ldots \quad .$$

In the same manner, the equations for the axial vibration, where no transverse deflections are allowed, can be found to be

(28) $$\ddot{v} = \frac{AE}{\rho} v_{rr} \qquad \text{B.C.} \Rightarrow v(0,t) = v(\ell,t) \equiv 0$$

and the frequencies of vibration are found to be

$$\omega_n = \frac{n\pi}{\ell}\sqrt{\frac{AE}{\rho}} \qquad n = 1, 2, \ldots \quad .$$

2. Case II - Spinning in Free Space

In order to study this case, we let $R = \infty$ as in Case I, but now specify that $\dot{\varphi} = \omega$ = constant and let the tension be a constant with respect to time but vary along the length of the cable. When the radial displacement is a function of r alone, it implies that the end mass is allowed to seek a steady state equilibrium position along the r,φ reference line and then is held fixed relative to that line for the remainder of the problem. This has the effect of eliminating the time dependent boundary conditions, since the position of the end mass is fixed in the rotating reference frame.

The following linearized equations result from equations (23) and (24)

$$v_{rr} + \frac{\rho\omega^2}{AE} v = -\frac{\rho\omega^2}{AE} r \tag{29}$$

and

$$\ddot{u} = u\omega^2 + \frac{AE}{\rho}(u_r v_{rr} + v_r u_{rr}) \tag{30}$$

where $\omega = \dot{\varphi} = \text{constant}$. The boundary conditions are

$$v(0,t) = u(0,t) \equiv 0$$

$$(\ell + v)\omega^2 - \frac{AE}{M} v_r = 0 \qquad r = \ell$$

and

$$u = 0 \qquad r = \ell$$

In order to solve the linear set, the Coriolis coupling terms have been neglected. This cannot be justified, since the Coriolis terms appear even in the linear equations. The equation which yields the steady state tension is equation (29) which has for solution

$$v(r) = B_1 \sin \alpha r + B_2 \cos \alpha r - r$$

where

$$\alpha = \sqrt{\frac{\rho\omega^2}{AE}} \ .$$

The boundary conditions for $v \ll \ell$ become

$$v(0,t) = 0 \text{ and } AEv_r(\ell,t) = M\omega^2\ell \quad \text{for } t \geq 0$$

which yields

$$B_2 = 0 \qquad \text{and} \qquad \alpha B_1 = \frac{1 + M\omega^2\ell/AE}{\cos \alpha\ell}$$

giving

$$\ddot{u} = u\omega^2 + \frac{AE}{\rho}\left[u_{rr}(\alpha B_1 \cos \alpha r - 1) - u_r\alpha^2 B_1 \sin \alpha r\right].$$

For $\alpha \ll 1$, i.e. small spin rates, we get

$$\alpha B_1 \cos \alpha r = \frac{\cos \alpha r}{\cos \alpha\ell}\left[1 + \frac{M\omega^2\ell}{AE}\right] \simeq \left[1 + \frac{\alpha^2}{2}(\ell^2 - r^2)\right]\left[1 + \frac{M\omega^2\ell}{AE}\right].$$

This is a reasonable assumption for the linear equations, since, as pointed out previously, nonlinear effects become important only as the spin rate becomes large. Hence we get

$$\ddot{u} = u\omega^2 + \frac{AE}{\rho}\left\{u_{rr}\left[\frac{\rho\omega^2}{2AE}(\ell^2 - r^2) + \frac{M\omega^2\ell}{AE}\right] - \frac{u_r\rho\omega^2 r}{AE}\right\}$$

or finally

$$\ddot{u} = u\omega^2 + \left\{u_{rr}\left[(\ell^2 - r^2) + \frac{M\ell}{\rho}\right] - u_r r\right\}\omega^2 . \tag{31}$$

To reiterate, the assumption of small displacements and slow spin rate have been made in order to linearize the equations.

Letting

$$u(r,t) = X(r)T(t)$$

yields

$$(32) \qquad \frac{\ddot{T}}{T} = -\beta^2 = \omega^2 + \frac{X_{rr}}{X}\left[-\frac{r^2}{2} + \frac{\ell^2}{2} + \frac{M\ell}{\rho}\right]\omega^2 - \frac{X_r}{X}r\omega^2$$

and

$$(33) \qquad X_{rr}\left(C - \frac{r^2}{2}\right)\omega^2 - r\omega^2 X_r + (\beta^2 + \omega^2)X = 0$$

where $C \equiv \ell^2\left[\frac{1}{2} + \frac{M}{\rho\ell}\right]$. If C is large, such as it would be for a large tip mass to cable weight ratio, and if we divide by C and neglect terms of order r/C, (33) reduces to

$$(34) \qquad X_{rr} + \frac{(\beta^2 + \omega^2)}{C\,\omega^2}X = 0$$

This is the vibrating string equation again, modified by the rotational rate ω^2. Hence

$$X(r) = B_1 \sin \alpha_1 r + B_2 \cos \alpha_1 r \qquad \text{where } \alpha_1 = \sqrt{\frac{\beta^2 + \omega^2}{C\,\omega^2}} \ .$$

The boundary conditions are $X(0) = 0$ and $X(\ell) = 0$ which gives

$$B_2 = 0 \qquad \text{and} \qquad \sin \alpha_1 \ell = n\pi$$

and

$$(34a) \qquad \beta^2 = \frac{\omega^2 C n^2 \pi^2}{\ell^2} - \omega^2 = \omega^2\left\{\frac{(n\pi)^2 M}{\rho\ell} - 1\right\} \ .$$

This shows that the frequency increases as (1) the spin rate increases, (2) the tip mass increases, or (3) cable mass, $\rho\ell$, decreases.

The effects of spinning and the effects of the corresponding tension increase can be separated as follows: from equation (30),

$$\ddot{u} = u\,\omega^2 + \frac{T}{\rho}\,u_{rr} \quad ,$$

for a constant tension which is not necessarily the steady state equilibrium tension

$$X_{rr} + \frac{\rho}{T}\,(\omega^2 + \beta^2)X = 0$$

and

$$X(r) = B_1 \sin \alpha_3 r \qquad \text{where} \qquad \alpha_3 = \sqrt{\frac{\rho}{T}\,(\omega^2 + \beta^2)} \quad ,$$

which gives

$$\beta^2 = \frac{T(n\pi)^2}{\rho\ell^2} - \omega^2 \qquad n = 1, 2, \ldots \quad .$$

This implies that for constant prescribed tension, spinning the system reduces the natural frequencies. If we substitute for T, its steady state equilibrium value, and we get

$$\beta^2 = \omega^2 \left[\frac{M}{\rho\ell}\,(n\pi)^2 - 1\right] \quad n = 1, 2, \ldots$$

which shows that spinning increases the natural frequencies if the tension is determined by the steady state equilibrium position of the end mass.

3. Case III - Spinning in Orbit

If we now let R be governed by the Keplerian equations of motion, $\dot{\varphi}$ be governed by the equations for a rigid rod spinning in orbit, the tension again be only a function of r, and neglect the Coriolis coupling, we can again separate variables and obtain solutions to the linearized equations. As pointed out for case II, neglecting the Coriolis coupling cannot be jus-

tified and may be a severe limitation on the results obtained by this analysis.

The steady state tension, AEv_r is governed by the following

$$\frac{\rho}{AE}(r + v)\left[\dot{\varphi}^2 + \frac{G}{2R^3}[1 + 3 \cos 2(\varphi - \theta)]\right] + v_{rr} = 0$$

with boundary conditions

$$AEv_r(\ell) = M\ell\left[\dot{\varphi}^2 + \frac{G}{2R^3}[1 + 3 \cos 2(\varphi - \theta)]\right] .$$

The expression for $v_r(r)$ which results is

$$v_r(r) = \left[AEM\ell + \frac{AE\rho}{2}(\ell^2 - r^2)\right]\left[\dot{\varphi}^2 + \frac{G}{2R^3}[1 + 3 \cos 2(\varphi - \theta)]\right] .$$

This and the expression for $v_{rr}(r)$ is substituted into (24) and then linearized to yield

$$(35) \quad \ddot{u} = u\left[\dot{\varphi}^2 + \frac{G}{2R^3}[1 - 3 \cos 2(\varphi - \theta)]\right] - r\left(\ddot{\varphi} - \frac{3G}{R^3} \sin 2(\varphi - \theta)\right)$$

$$+ \left[u_{rr}\left(\frac{\ell^2 - r^2}{2} + \frac{M\ell}{\rho}\right) - u_r r\right]\left[\dot{\varphi}^2 + \frac{G}{2R^3}[1 + 3 \sin 2(\varphi - \theta)]\right] .$$

Equation (35) is the same as equation (31) if $R = \infty$, and $\dot{\varphi} = \omega$, and $\ddot{\varphi} = 0$. The mode shapes can be obtained for certain simplified cases as shown for the free space solution of equation (31).

The corresponding time varying equation, after separating variables, is of the form

$$(36) \qquad \ddot{T} + \left(\beta + \epsilon f(t)\right)T = 0 \quad .$$

The details of the separation of variable will not be shown here, since only the general form of the time dependent function, T(t), is discussed. In order that separation of variables be applicable, we must have

$$\ddot{\varphi} = \frac{3G}{R^3} \sin 2(\varphi - \theta) = \dot{\varphi} \frac{d\dot{\varphi}}{d\varphi}$$

$$\text{or} \quad (\dot{\varphi})^2 = -\frac{3G}{2R^3} \cos 2(\varphi - \theta) + [\dot{\varphi}(0)]^2 \quad .$$

This differential equation governs the variation of φ for the reference frame and introduces the time dependency, f(t), into equation (36). The above equation for φ is the equation for a rigid dumbbell in orbit. If the length of the dumbbell is assumed to be a constant, the equation may be obtained from the equations for an elastic dumbbell which are derived in chapter IV. Equation (35) and the form of equation (36) agree with those derived by Targoff [7].

Targoff discusses stability for $\omega \geq 3\dot{\theta}$ where he shows that equation (36) can be approximated by the Mathieu equation. He concludes that the system is unstable in some cases but that a small amount of damping will stabilize the motion.

It is questionable whether sufficient damping will be present for small deflections. As will be demonstrated in chapter III, including viscous damping in the equations for the cable does not produce linear terms in the equations for the transverse motion as it does in the equations for the axial motion and, hence, does not yield the desired damping effect. Flexural damping would certainly help, but the curvatures involved are so large for linear deflections of long thin cables that the flexural damping present would also be negligible.

Many approximations have been made in order to achieve a solution and the effects of these assumptions are difficult to assess. Even a numerical integration of the complete equations would be difficult due to the time dependent boundary conditions. Furthermore, if complex structures are to be studied, there seems to exist no method of stability determination that can serve as a design procedure.

However, a system such as the one discussed can be approximated by point masses and massless springs. The advantage offered is that the stability properties of the resulting equations of motion have been extensively studied.

CHAPTER III

LUMPED MASS MODEL

In this chapter, the exact equations of motion for the lumped system are derived using Lagrange's method. Viscous damping terms are also derived for the lumped system for the case where the neighboring mass points have velocity dependent dampers between them. These equations were numerically integrated and the results appear in a later chapter.

The continuous system in Figure 1 can be approximated by a number of mass points connected by linear elastic massless springs as shown in Figure 2.

The Lagrangian for this model is now a function of the variables ℓ_i, φ_i, $\dot{\ell}_i$, $\dot{\varphi}_i$, t. The equations of motion are given by

$$\frac{d}{dt}\left[\frac{\partial L}{\partial \dot{q}_i}\right] - \frac{\partial L}{\partial q_i} = Q_i \qquad i = 1, 2, \ldots, n+1.$$

From the continuous analysis, we showed that certain terms from the kinetic energy contribution to the Lagrangian canceled with the first term from the expansion of the gravity potential contribution when the center of mass moved in a Keplerian orbit. This fact will be demonstrated in the developments of the equations for the simple models that follow.

The kinetic energy is

$$T = \frac{1}{2} M_T[\dot{R}^2 + (R\dot{\theta})^2] + \frac{1}{2}\sum_{i=1}^{n+1} M_i[\dot{\ell}_i^2 + (\ell_i\dot{\varphi}_i)^2]$$

where M_T = total mass of system $= \sum_{i=1}^{n+1} M_i$.

The magnitude of the vector from the center of the Earth to the i^{th} mass is given by

$$|\bar{r}_i| = \sqrt{R^2 + \ell_i^2 + 2R\ell_i \cos(\varphi_i - \theta)} \quad . \tag{37}$$

The length of the spring between mass $i-1$ and i, from the law of cosines, is

$$e_i = \sqrt{\ell_{i-1}^2 + \ell_i^2 - 2\ell_i\ell_{i-1} \cos(\varphi_{i-1} - \varphi_i)} \quad .$$

If we define the unstretched length of each spring as ℓ_{i0}, the elastic potential may be written as

$$V_E = \frac{1}{2}\sum_{i=1}^{n+1} k_i [e_i - \ell_{i0}]^2$$

where k_i is the spring constant of the i^{th} spring. The gravity potential in expanded form is

$$V_G = -G\sum_{i=1}^{n+1}\left\{\frac{M_i}{R}\left[1 - \frac{\ell_i \cos(\varphi_i - \theta)}{R} - \frac{\ell_i^2}{2R^2}[1 - 3\cos^2(\varphi_i - \theta)] + \mathcal{O}\left(\frac{\ell_i^3}{R^3}\right)\right]\right\} \quad .$$

The Lagrangian is $L = T - V_E - V_G$. We will now proceed to compute the necessary derivatives, namely

$$\frac{\partial L}{\partial \dot{\ell}_j} = M_j \dot{\ell}_j \qquad \text{and} \qquad \frac{d}{dt}\left[\frac{\partial L}{\partial \dot{\ell}_j}\right] = M_j \ddot{\ell}_j$$

$$\frac{\partial L}{\partial \ell_j} = M_j\left\{\ell_j \dot{\varphi}_j^2 - \frac{k_j + 1}{M_j}\left(1 - \frac{\ell_{(j+1)0}}{e_{j+1}}\right)[\ell_j - \ell_{j+1}\cos(\varphi_j - \varphi_{j+1})]\right.$$

$$- \frac{k_j}{M_j}\left(1 - \frac{\ell_{j0}}{e_j}\right)[\ell_j - \ell_{j-1}\cos(\varphi_{j-1} - \varphi_j)]$$

$$\left. - \left(\frac{G\ell_j}{2R^3}\right)[1 + 3\cos 2(\varphi_j - \theta]\right\}$$

$$\frac{\partial L}{\partial \dot{\varphi}_j} = M_j \ell_j^2 \dot{\varphi}_j \qquad \text{and} \qquad \frac{d}{dt}\left[\frac{\partial L}{\partial \dot{\varphi}_j}\right] = 2M_j \ell_j \dot{\ell}_j \dot{\varphi}_j + M_j \ell_j^2 \ddot{\varphi}_j$$

$$\frac{\partial L}{\partial \varphi_j} = M_j\left\{-\frac{k_j + 1}{M_j}\left(1 - \frac{\ell_{(j+1)0}}{e_{j+1}}\right)[\ell_j \ell_{j+1}\sin(\varphi_j - \varphi_{j+1})]\right.$$

$$\left. + \frac{k_j}{M_j}\left(1 - \frac{\ell_{j0}}{e_j}\right)[\ell_j \ell_{j-1}\sin(\varphi_j - \varphi_{j-1})] + \frac{3G\ell_j}{2R^3}\sin 2(\varphi_j - \theta)\right\}.$$

Hence, the general equations of motion are

$$(38)\quad \ddot{\ell}_j = \ell_j\dot{\varphi}_j^2 - \frac{k_{j+1}}{M_j}\left(1 - \frac{\ell_{(j+1)0}}{e_{j+1}}\right)[\ell_j - \ell_{j+1}\cos(\varphi_j - \varphi_{j+1})]$$

$$- \frac{k_j}{M_j}\left(1 - \frac{\ell_{j0}}{e_j}\right)[\ell_j - \ell_{j-1}\cos(\varphi_{j-1} - \varphi_j)]$$

$$+ \frac{G\ell_j}{2R^3}[1 + 3\cos 2(\varphi_j - \theta)]$$

and

$$(39)\quad \ddot{\varphi}_j = -\frac{2\dot{\ell}_j\dot{\varphi}_j}{\ell_j} - \frac{k_{j+1}}{M_j}\left(1 - \frac{\ell_{(j+1)0}}{e_{j+1}}\right)\left[\frac{\ell_{j+1}}{\ell_j}\sin(\varphi_j - \varphi_{j+1})\right]$$

$$+ \frac{k_j}{M_j}\left(1 - \frac{\ell_{j0}}{e_j}\right)\left[\frac{\ell_{j-1}}{\ell_j}\sin(\varphi_{j-1} - \varphi_j)\right] - \frac{3G}{2R^3}\sin 2(\varphi_j - \theta)$$

$j = 1, 2, \ldots, n+1$.

The following definitions will account for the end conditions

$$\ell_0 = 0 \qquad \text{and} \qquad k_{n+2} = 0 \quad .$$

These two definitions will yield the proper system of equations for the subsatellite-cable model considered here. The Lagrangian derived above will have the same form for any system of particles connected by linear elastic, massless springs. The only change will be the elastic potential. Its form will depend on the manner in which the system is tied together, but the method of derivation is unchanged.

At this point, let us examine how damping may be put into equations (38) and (39). If we consider viscous (i.e. velocity dependent) damping, the force may be written as

$$F_{DAMP} = - C_i \dot{e}_i$$

where $C_i \equiv$ damping factor of i^{th} spring whose rate of change of length is $\dot{e}_i$. From our previous calculations of e_i, we can derive

$$(40)\quad \dot{e}_i = \frac{\dot{\ell}_{i-1}\ell_{i-1} + \dot{\ell}_i\ell_i - [\ell_i\dot{\ell}_{i-1} + \dot{\ell}_i\ell_{i-1}] \cos(\varphi_{i-1} - \varphi_i)}{e_i}$$

$$+ \frac{\ell_i\ell_{i-1}(\dot{\varphi}_{i-1} - \dot{\varphi}_i) \sin(\varphi_{i-1} - \varphi_i)}{e_i} \quad .$$

In Lagrange's equation of motion, this contribution is treated as a generalized force since it is non-conservative. The virtual work done by the generalized force is

$$Q_i \delta q_i = [\text{component of } (C_i \dot{e}_i) \text{ along } q_i]\, \delta q_i$$

(where Q_i must be a moment if q_i is an angular coordinate. In this case, the q_i's are the ℓ_i's and φ_i's. We now turn to the geometry of the problem

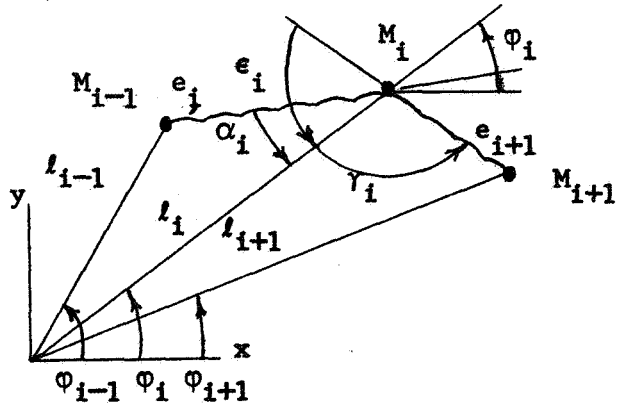

From the law of sines

$$\frac{\sin \alpha_i}{\ell_{i-1}} = \frac{\sin (\varphi_{i-1} - \varphi_i)}{e_i} \quad .$$

The components of $C_i \dot{e}_i$ along ℓ_i and normal to ℓ_i are

$$- C_i \dot{e}_i \cos \alpha_i \qquad \text{and} \qquad - C_i \dot{e}_i \sin \alpha_i$$

respectively. The contribution of $C_{i+1} \dot{e}_{i+1}$ is

$$- C_{i+1} \dot{e}_{i+1} \cos \epsilon_i \quad \text{and} \quad - C_{i+1} \dot{e}_{i+1} \sin \epsilon_i$$

where

$$\epsilon_i = 180° - \gamma_i \qquad \text{and} \qquad \sin \gamma_i = \frac{\sin (\varphi_i - \varphi_{i+1})}{e_{i+1}} \ell_{i+1}$$

Thus, in equation (38), the following terms must be added to the right-hand side if damping is to be considered

$$(41) \quad - \frac{C_j}{M_j} \left\{ \frac{\dot{\ell}_{j-1} \ell_{j-1} + \dot{\ell}_j \ell_j - [\ell_j \dot{\ell}_{j-1} + \dot{\ell}_j \ell_{j-1}] \cos (\varphi_{j-1} - \varphi_j)}{e_j} \right.$$

$$\left. + \frac{\ell_j \ell_{j-1} (\dot{\varphi}_{j-1} - \dot{\varphi}_j) \sin (\varphi_{j-1} - \varphi_j)}{e_j} \right\} \cos \alpha_j$$

$$- \frac{C_{j+1}}{M_j} \left\{ \frac{\dot{\ell}_j \ell_j + \dot{\ell}_{j+1} \ell_{j+1} - [\ell_{j+1} \dot{\ell}_j + \dot{\ell}_{j+1} \ell_j] \cos (\varphi_j - \varphi_{j+1})}{e_{j+1}} \right.$$

$$\left. + \frac{\ell_{j+1} \ell_j (\dot{\varphi}_j - \dot{\varphi}_{j+1}) \sin (\varphi_j - \varphi_{j+1})}{e_{j+1}} \right\} \cos \epsilon_j$$

and for equation (39)

$$(42) \quad -\frac{C_j}{\ell_j M_j}\left\{\text{same as first term in (41)}\right\}\sin\alpha_j$$

$$-\frac{C_{j+1}}{\ell_j M_j}\left\{\text{same as second term in (41)}\right\}\sin\epsilon_j \quad .$$

Now that the complete nonlinear equations of motion for a lumped mass model have been derived, the next step would be to consider the simplest case and gradually increase the complexity. However, before this is begun, the effect of the expansion of the gravity potential which uncouples the relative motion from the orbital motion will be examined. To do this we examine the dumbbell model shown in Figure 3.

1. Dumbbell Model

Thus far in the analysis, the center of rotation of the relative motion has been assumed to move in an undisturbed Keplerian orbit. There is, however, a coupling between the relative motion and the orbital motion such that the orbit cannot be exactly Keplerian. The purpose of this chapter is to show what bounds exist in the center of mass motion and also to show that the assumption that the center of mass moving in an undisturbed Keplerian orbit will produce errors which are of the order of the errors which result from a single precision numerical analysis.

The essence of gravity gradient effects on finite, non-axisymmetric bodies in orbit can best be shown by starting with a simple two mass dumbbell model (Figure 3). The two masses are connected by a massless, linear elastic spring. The exact equations of motion can be derived by

using Lagrange's equation. For the dumbbell model shown in Figure 3, the angle φ can be measured from either the nonrotating x axis or from the local vertical. The former provides a slightly simpler form of the equations while the latter allows one to derive the conservation of angular momentum equations more directly. There is, however, no clear cut reason for prefering either one of the two coordinate systems over the other.

For the dumbbell model shown in Figure 3 and measuring φ relative to the x axis, the kinetic energy and potential energy are respectively

$$T = M[\dot{R}^2 + (R\dot{\theta}^2) + \dot{\ell}^2 + (\ell\dot{\varphi})^2] \tag{43}$$

and

$$V = -GM\left\{[R^2 + \ell^2 + 2R\ell\cos(\theta - \varphi)]^{-1/2} + [R^2 + \ell^2 - 2R\ell\cos(\theta - \varphi)]^{-1/2}\right\} + k(\ell - \ell_0)^2 \tag{44}$$

where G = product of universal gravitational constant and mass of Earth

k = spring constant

M = end mass.

The resulting equations of motion are

Orbital radius

$$\ddot{R} = R\dot{\theta}^2 - \frac{G}{2}\left\{\frac{R + \ell\cos(\theta - \varphi)}{A} + \frac{R - \ell\cos(\theta - \varphi)}{B}\right\} \tag{45}$$

Orbital angle

$$\ddot{\theta} = -\frac{2\dot{R}\dot{\theta}}{R} + \frac{G\ell\sin(\theta - \varphi)}{2R}\left\{\frac{1}{A} - \frac{1}{B}\right\} \tag{46}$$

Relative angle

$$(47)\quad \ddot{\varphi} = -\frac{2\dot{\ell}\dot{\varphi}}{\ell} - \frac{GR \sin(\theta - \varphi)}{2\ell}\left\{\frac{1}{A} - \frac{1}{B}\right\}$$

Spring half-length

$$(48)\quad \ddot{\ell} = \ell\dot{\varphi}^2 - \frac{G}{2}\left\{\frac{\ell + R\cos(\theta - \varphi)}{A} + \frac{\ell - R\cos(\theta - \varphi)}{B}\right\} - \frac{k}{M}(\ell - \ell_0)$$

where

$$A = [R^2 + \ell^2 + 2R\ell\cos(\theta - \varphi)]^{3/2} \quad \text{and} \quad B = [R^2 + \ell^2 - 2R\ell\cos(\theta - \varphi)]^{3/2}.$$

The coordinate system taken with φ measured from the local vertical to the Earth yields slightly different equations. The Lagrangian is now given by

$$(49)\quad L = M[\dot{R}^2 + (R\dot{\theta})^2 + \dot{\ell}^2 + \ell^2(\dot{\varphi} + \dot{\theta})^2] + MG\left\{[R^2 + \ell^2 + 2R\ell\cos\varphi]^{-1/2} + [R^2 + \ell^2 - 2R\ell\cos\varphi]^{-1/2}\right\} - k(\ell - \ell_0)^2$$

and the equations are

Orbital radius

$$(50)\quad \ddot{R} = R\dot{\theta}^2 - \frac{G}{2}\left\{\frac{R + \ell\cos\varphi}{A'} + \frac{R - \ell\cos\varphi}{B'}\right\}$$

Orbital angle

$$(51)\quad \frac{d}{dt}\left\{2M[R^2\dot{\theta} + \ell^2(\dot{\varphi} + \dot{\theta})]\right\} = 0$$

Relative angle

$$(52)\quad \ddot{\varphi} = -\ddot{\theta} - \frac{2\dot{\ell}(\dot{\varphi} + \dot{\theta})}{\ell} + \frac{GR}{2\ell} \sin\varphi \left\{\frac{1}{A'} - \frac{1}{B'}\right\}$$

Spring half-length

$$(53)\quad \ddot{\ell} = \ell(\dot{\varphi} + \dot{\theta})^2 - \frac{G}{2}\left\{\frac{\ell + R\cos\varphi}{A'} + \frac{\ell - R\cos\varphi}{B'}\right\} - \frac{k}{M}(\ell - \ell_0)$$

where

$$A' = [R^2 + \ell^2 + 2R\ell\cos\varphi]^{3/2} \quad \text{and} \quad B' = [R^2 + \ell^2 - R\ell\cos\varphi]^{3/2} .$$

As stated above, the advantage of this coordinate system is that the conservation of angular momentum can be seen directly from equation (51). This happens because in this coordinate system, θ is a cyclic coordinate, that is, a rotation of the reference for θ does not change the value of the Lagrangian.

However, the conservation of angular momentum can also be seen for the original system after some manipulation. Multiply equation (46) by $\frac{R}{\ell}$ and (47) by ℓ/R and add the resulting equations to get

$$(54)\qquad \frac{R\ddot{\theta}}{\ell} + \frac{\ell\ddot{\varphi}}{R} + \frac{2R\ddot{\theta}}{\ell} + \frac{2\ell\ddot{\varphi}}{R} = 0$$

or

$$\frac{d}{dt}\left\{R^2\dot{\theta} + \ell^2\dot{\varphi}\right\} = 0$$

which is the equation for conservation of angular momentum. Either coordinate system may be used for the analysis. The second system, where θ is cyclic, facilitates the energy analysis that follows while

the simpler form of the equations resulting from use of the first system may simplify the numerical analysis somewhat.

For the second system we can eliminate $\dot{\theta}$ from the total energy as follows: let H be the angular momentum of the system, then for equation (51) we get

$$\dot{\theta}(R^2 + \ell^2) + \ell^2\dot{\varphi} = \frac{H}{2M} \tag{55}$$

or

$$\dot{\theta} = \frac{\left\{-\ell^2\dot{\varphi} + \frac{H}{2M}\right\}}{(R^2 + \ell^2)} \tag{56}$$

This expression for $\dot{\theta}$ is now put into the expression for the total energy, E_0, which also is a constant since the system is conservative and has no external forces

$$E_0 = T + V$$

hence

$$E_0 = M\left[\dot{R}^2 + \frac{R^2(-\ell^2\dot{\varphi} + H/2M)^2}{(R^2 + \ell^2)^2} + \dot{\ell}^2 + \ell^2\left(\dot{\varphi} + \frac{(-\ell^2\dot{\varphi} + H/2M)}{(R^2 + \ell^2)^2}\right)^2\right]$$

$$- MG\left\{[R^2 + \ell^2 + 2R\ell\cos\varphi]^{-1/2} + [R^2 + \ell^2 - 2R\ell\cos\varphi]^{-1/2}\right\}$$

$$+ k(\ell - \ell_0)^2 \quad .$$

Collecting terms which are positive definite yields

$$T_0 = M\left\{\dot{R}^2 + \dot{\ell}^2 + \frac{(\ell\dot{\varphi})^2}{1 + (\frac{\ell}{R})^2}\right\} + k(\ell - \ell_0)^2 \geq 0$$

and the fictitious potential V_0. It is called fictitious because it contains terms which come from the kinetic energy term. However, it may be treated as a potential function. We get,

$$(57)\quad V_0 = \frac{H^2}{4M(R^2 + \ell^2)} - MG\left\{\frac{1}{(R^2 + \ell^2 + 2R\ell\cos\varphi)^{1/2}} + \frac{1}{(R^2 + \ell^2 - 2R\ell\cos\varphi)^{1/2}}\right\}$$

but

$$E_0 = T_0 + V_0 \qquad \text{and} \qquad V_0 = E_0 - T_0$$

or

$$V_0 \leq E_0 \qquad \text{since} \qquad T_0 \geq 0\ .$$

Note that for $\ell \equiv 0$, we get

$$(58)\qquad V_0 = \frac{H^2}{4MR^2} - \frac{2MG}{R}\ .$$

Equation (58) is the fictitious potential derived for a point with mass 2M in an inverse square attraction field as shown in Goldstein[12]. If we expand the fictitious potential (57) in terms of the ratio of the body dimension to orbital radius, namely ℓ/R, we get

$$V_0 = \frac{H_0^2}{4MR^2}\left[1 + \left(\frac{\ell}{R}\right)^2 + \mathcal{O}\left(\frac{\ell}{R}\right)^4\right] - \frac{MG}{R}\left\{1 - \frac{1}{2}\left[\left(\frac{\ell}{R}\right)^2 + \frac{2\ell}{R}\cos\varphi\right] + \right.$$

$$+\frac{3}{8}\left[4\left(\frac{\ell}{R}\right)^2\cos^2\varphi\right]+\mathcal{O}\left(\frac{\ell}{R}\right)^3\Big\}-\frac{MG}{R}\Big\{1-\frac{1}{2}\left[\left(\frac{\ell}{R}\right)^2-\frac{2\ell}{R}\cos\varphi\right]$$

$$+\frac{3}{8}\left[4\left(\frac{\ell}{R}\right)^2\cos^2\varphi\right]+\mathcal{O}\left(\frac{\ell}{R}\right)^3\Big\}$$

or

$$V_0 \doteq \left[\frac{H_0^2}{4MR^2}-\frac{2MG}{R}\right]+\left(\frac{\ell}{R}\right)^2\left\{\frac{H_0^2}{4MR^2}-\frac{MG}{2R}\left[1+3\cos 2\varphi\right]\right\} \quad .$$

As expected, the first term is the term in (58) for a point mass and the second term is the perturbation due to the finite size of the body. When this potential function is plotted versus R for a fixed φ, the shape of the potential "well" is essentially no different from that for a point mass. This is because $(\ell/R)^2$ is of the order of 10^{-6} even for a body with dimensions of the order of miles. This potential can also be plotted versus the relative angle φ. Relative minima are found when

$$\frac{\partial V_0}{\partial \varphi}=0 \qquad \text{and} \qquad \frac{\partial^2 V_0}{\partial \varphi^2}>0$$

where

$$\frac{\partial V_0}{\partial \varphi}=3\left(\frac{\ell}{R}\right)^2\frac{MG}{R}\sin 2\varphi$$

and is zero at

$$\varphi = 0, \pm\frac{\pi}{2}, \pm\pi, \ldots$$

$$\frac{\partial^2 V_0}{\partial \varphi^2} = 3\left(\frac{\ell}{R}\right)^2 \frac{MG}{R} \cos 2\varphi$$

which is greater than zero when

$$\varphi = 0, \pm \pi, \pm 2\pi, \ldots$$

and is less than zero when

$$\varphi = \pm \frac{\pi}{2}, \pm \frac{3\pi}{2}, \ldots$$

Thus, the dumbbell is stable for a circular orbit when $\frac{\partial^2 V_0}{\partial \varphi^2} > 0$ or, as expected, when the dumbbell points directly towards the Earth. This analysis also shows that when the dumbbell is pointed normal to the radius from the Earth's center, the position is unstable.

If the system is not in a circular or nearly circular orbit, the upper bound on the energy is higher up the sides of the potential well and a conclusion about gravity gradient stabilization cannot be reached by this analysis. This corresponds to an elliptic orbit, for which the orbital angular rate changes periodically. The dumbbell cannot stabilize itself about the local vertical for other than circular or nearly circular orbits due to this changing orbital angular rate. It is entirely possible that the system could continue to increase its spin rate while the orbit decayed to a circular orbit. This would correspond to starting at the top of the energy bounds in the potential well and the moving down towards the bottom of the well while the orbit lost energy and the relative motions gained energy through an increased spin rate. It can be concluded that if this possible increase in spin rate is undesirable from a

design viewpoint, the system should be placed in a circular orbit.

The actual motion of the spinning elastic dumbbell in orbit was found for certain initial conditions and parameters by numerically integrating equations (45) through (48). A fourth order Runge-Kutta technique was used with double precision arithmetic on an IBM 7090 digital computer.

Figure 4 shows a typical plot of the deviation of the orbital radial distance for the dumbbell from a Keplerian orbit having the same initial conditions. Figure 5 shows the corresponding spin rate, φ, measured from the nonrotating coordinate system shown in Figure 3. Note that the spin rate is drastically reduced as it passes through perigee and, even at the next apogee, it has not recovered its spin rate. Since total energy is conserved, the loss represented by the slower spin rate must show up as a movement of the center of mass to a higher energy orbit. Figure 4 shows that this is precisely what happens. The radial distance is as much as 108 feet longer after passing perigee. Other cases were found where the spin rate increased during perigee passage and the radial distance decreased accordingly. This exchange of energy from the orbit to the relative motion would be destructive if it were to continue indefinitely. The change in radial distance is quite small compared to the distance itself and the relative motion is unaffected by these changes for the time interval of most computations.

As a consequence of the above results, equations (45) through (48) were also expanded in terms of (ℓ/R) and only first order terms retained. The resulting equations are

Orbit

$$(59)\quad \ddot{R} = R\dot{\theta}^2 - \frac{G}{R^2} \qquad \text{and} \qquad (60)\quad \ddot{\theta} = -\frac{2\dot{R}\dot{\theta}}{R}$$

Relative motion

$$(61) \qquad \ddot{\ell} = \ell\dot{\varphi}^2 + \frac{G\ell}{2R^3}\left[1 + 3\cos 2(\phi - \theta)\right] - \frac{k}{M}(\ell - \ell_0)$$

and

$$(62) \qquad \ddot{\varphi} = -\frac{2\dot{\ell}\dot{\varphi}}{\ell} - \frac{3G}{2R^3}\sin 2(\varphi - \theta) \quad .$$

The effect of the expansion and dropping of higher order terms is to uncouple the relative motion from the orbital motion as mentioned previously. Equations (59) and (60) are those for a point mass in orbit. Equations (61) and (62) are those of an elastic dumbbell in free space plus an additional term in each equation from the gravity gradient.

These equations were also numerically integrated as was the previous set of equations except that single precision arithmetic was used. A comparison was made between the relative motion calculated using the exact equations (45) through (48) and the expanded set shown above, (59) through (62). The two calculations agreed to within five significant figures and the differences appeared to be due to round-off for the single precision cases. This seems to justify the use of the expanded form of the equations for numerical computations, even if the system is in an elliptic orbit.

2. Single Mass Model

An alternate simple spring mass model to be analyzed is a light end mass attached to a much heavier mass by a linear elastic, massless spring as shown in Figure 6. This is the simplest lumped mass model which

approximates the original distributed mass system shown in Figure 1. It will be shown below that the equations of this single mass model and those of the dumbbell are identical to terms of order $(\ell/R)^2$. The Lagrangian for this case is

$$(63)\quad L = \frac{M}{2}\left\{\dot{R}^2 + (R\dot{\theta})^2 + \dot{\ell}^2 + (\ell\dot{\varphi})^2 + [2R\ddot{\ell} + 2R\dot{\theta}\ell\dot{\varphi}]\cos(\varphi-\theta) + \sin(\varphi-\theta)[2R\theta\ddot{\ell} - 2R\dot{\ell}\dot{\varphi}]\right\} + \frac{GM}{\left(R^2 + \ell^2 + 2R\ell\cos(\varphi-\theta)\right)^{1/2}} - \frac{k}{2}(\ell-\ell_0)^2 \quad .$$

However, if the equations of motion for ℓ and φ are derived and expanded in terms of ℓ/R as before, we get

$$(64)\quad \ddot{\ell} - \ell\dot{\varphi}^2 - \frac{G\ell}{2R^3}[1 + 3\cos 2(\varphi-\theta)] + \frac{k}{M}(\ell-\ell_0) = -\left(\ddot{R} - R\dot{\theta}^2 + \frac{G}{R^2}\right)\cos(\varphi-\theta) - \left(R\ddot{\theta} + 2\dot{R}\dot{\theta}\right)\sin(\varphi-\theta)$$

and

$$(65)\quad \ddot{\varphi} + \frac{2\dot{\ell}\dot{\varphi}}{\ell} + \frac{3G}{2R^3}\sin 2(\varphi-\theta) = \left(\ddot{R} - R\dot{\theta}^2 + \frac{G}{R^2}\right)\frac{\sin(\varphi-\theta)}{\ell} - \left(R\ddot{\theta} + 2\dot{R}\dot{\theta}\right)\frac{\cos(\varphi-\theta)}{\ell} \quad .$$

These equations differ from (61) and (62) only by the two terms on the right-hand side which are, however, zero for a Keplerian orbit. Thus,

equations (64) and (65) are exactly the same as those for the dumbbell (61) and (62).

The consequence of this is that one can consider either a dumbbell or a single mass connected to a much heavier mass. The equations of motion are identical if terms of the order of $(\ell/R)^2$ are neglected. This could also have been shown directly from the Lagrangian for the dumbbell, equations (43) and (44). If the potential, V, were expanded in terms of ℓ/R, it would be seen to be independent of rotations in $(\varphi - \theta)$ equal to $n\pi$. In other words, the dumbbell has the same motion (to order ℓ/R) independent of whether it was initially started at $\varphi = \varphi_i$ or $\varphi_i + n\pi$.

These equations expanded in terms of ℓ/R are still nonlinear and do not readily yield a solution. The usual procedure is to linearize the nonlinear equations about some stationary point to determine the motion and stability in the neighborhood of the point. A stationary point is an exact solution to the nonlinear set of equations for which the accelerations or second order derivatives are identically zero. One stationary point for the above system corresponds to gravity gradient stabilization.

3. Single Mass Model, Gravity Gradient Stabilized

As has been shown before, in circular or near circular orbits, the system is in a bounded potential well and must be stable in the sense that oscillations may exist but may not grow without bound. The nature of this motion can also be shown by examining the linearized equations. As the desired reference state, we choose

$$\ell_s = \text{const}, \; R = \text{const}, \; \dot{\theta} = \dot{\varphi}_0 = \text{const}, \text{ and } \varphi_0 = \theta_0 \quad .$$

Thus, we get for equations (61) and (62), where q_1 and q_2 are the deviations from the reference state, ℓ_s and φ_0 respectively,

$$(66)\quad \ddot{q}_1 = \left[\dot{\varphi}_0^2 - \frac{k}{M} + \frac{2G}{R^3}\right]q_1 + 2\ell_s\dot{\varphi}_0\dot{q}_2 + \frac{2G\ell_s}{R^3} + \ell_s\dot{\varphi}_0^2 - \frac{k}{M}(\ell_s - \ell_0)$$

and

$$(67)\quad q_2 = \frac{-2\dot{\varphi}_0}{\ell_s}\dot{q}_1 - \frac{3G}{R^3}q_2 \quad .$$

These can be simplified by choosing the stretched length,

$$(68)\quad \ell_s = \frac{\frac{k}{M}\ell_0}{(\frac{k}{M} - 3\dot{\theta}^2)} \quad ,$$

which is the stretched equilibrium length of the rotating spring, and noting that

$$\dot{\theta}^2 = \frac{G}{R^3} = \dot{\varphi}_0^2$$

which leaves

$$(69)\quad \ddot{q}_1 = -\left[\frac{k}{M} - 3\dot{\theta}^2\right]q_1 + 2\ell_s\ddot{\theta}q_2$$

and

$$(70)\quad \ddot{q}_2 = \frac{-2\dot{\theta}}{\ell_s}\dot{q}_1 - 3\dot{\theta}^2 q_2 \quad .$$

The characteristic exponents for a <u>rigid</u> dumbbell for which $q_1 \equiv 0$, are

$$\lambda = \pm i\sqrt{3}\,\dot{\theta} \quad .$$

Thus, the motion is periodic with a frequency of $\sqrt{3}\,\dot{\theta}$. This agrees with the frequency found by Paul[1]. The frequencies for equations (69) and (70) are

$$(71) \qquad \lambda = \pm i \sqrt{\frac{\left|\frac{k}{M} + 4\dot{\theta}^2\right|}{2} - \sqrt{\frac{\left|\frac{k}{M}\right|^2 - 4\dot{\theta}^2\,\frac{k}{M} + 52\dot{\theta}^4}{2}}}$$

and

$$(72) \qquad \pm i \sqrt{\frac{\left|\frac{k}{M} + 4\dot{\theta}^2\right|}{2} + \sqrt{\frac{\left|\frac{k}{M}\right|^2 - 4\dot{\theta}^2\,\frac{k}{M} + 52\dot{\theta}^4}{2}}}$$

From equation (68) for the steady state length of the spring, we can see the k/M must be larger than $3\dot{\theta}^2$ for a physically realizable result. If $k/M \gg \dot{\theta}^2$, we can expand the inner radical in equations (71) and (72) and show the orbital effects on the natural frequencies. After expanding, one gets

$$(73) \qquad \lambda = \pm i\sqrt{3}\,\dot{\theta} \qquad \text{and} \qquad \pm i\sqrt{\frac{k}{M} + 3\dot{\theta}^2} \quad .$$

The first root is the same as that of the rigid dumbbell while the second is the natural frequency of the nonspinning spring mass system except for the additional term, $3\dot{\theta}^2$, which effectively "stiffens" the system.

Let us now examine the stability of the dumbbell moving so as to always have its axis tangent to its orbital path. For this case,

$$\varphi_i = \theta_i + \pi/2$$

and we get for the linearized equations

$$\ddot{q}_1 = -\left[\frac{k}{M} - \frac{\dot{\theta}^2}{2}\right] q_1 + 2\ell_s \dot{\varphi}_0 \dot{q}_2 - \frac{3G\ell_s}{R^3} q_2 \tag{73}$$

and

$$\ddot{q}_1 = -\frac{2\dot{\varphi}_0}{\ell_s} \dot{q}_1 - \frac{3G}{2R^3} \tag{74}$$

where ℓ_s is given by

$$\ell_s = \frac{\frac{k}{M}\ell_0}{\left(\frac{k}{M} - \frac{3}{2}\dot{\theta}^2\right)} .$$

The corresponding characteristic equation is

$$\lambda\left[\lambda^3 + \left(\frac{k}{M} + \frac{7\dot{\theta}^2}{2}\right)\lambda - 6\dot{\theta}^3\right] = 0 . \tag{75}$$

One root is obviously zero. For the remaining cubic, if

$$9\dot{\theta}^6 + \frac{\left(\frac{k}{M} + \frac{7\dot{\theta}^2}{2}\right)}{27} > 0$$

there will be one real root and two conjugate complex roots. A necessary condition for the one real root of (75) to be negative, and, hence, yield a stable solution, would be for all the coefficients of (75) to be of the same sign and non-zero. This is not the case; therefore, the solution is unstable as was shown by examining the potential.

4. Single Mass Model Spinning in Orbit

The next item to be discussed is the stability and motion of the dumbbell spinning in orbit. Equations (59) through (62) apply and can be linearized. However, since the system is spinning, $(\varphi - \theta)$ is not a constant and the additional nonlinear term results from the sine and cosine terms in (61) and (62). Furthermore, there is no longer a stationary point about which to linearize. A stationary point exists for the spinning system only in the limit as $R \to \infty$ in which case the equations become those for an elastic dumbbell in free space, namely,

$$\ddot{\ell} = \ell\dot{\varphi}^2 - \frac{k}{M}(\ell - \ell_0) \tag{76}$$

and

$$\ddot{\varphi} = -\frac{2\dot{\ell}\dot{\varphi}}{\ell} \quad \text{or} \quad \frac{d}{dt}(\ell^2\dot{\varphi}) = 0 \; . \tag{77}$$

A stationary point is given by

$$\ell_s = \text{const. and } \dot{\varphi}_0 = \text{const.}$$

Thus, we define the stretched length of the spring, ℓ_s, at $R = \infty$ to be the free space stretched equilibrium length

$$\ell_s = \frac{\frac{k}{M}\ell_0}{\left[\frac{k}{M} - \dot{\varphi}^2\right]} \; .$$

We may now linearize equations (76) and (77) about these reference motions. By defining

$$\ell = \ell_s + q_1 \quad \text{and} \quad \varphi = \varphi_0 + q_2$$

we get

$$\ddot{q}_1 = -\left[\frac{k}{M} - \dot{\varphi}_0^2\right] q_1 + 2\ell_s \dot{\varphi}_0 \dot{q}_2 \tag{78}$$

and

$$\ddot{q}_2 = -\frac{2\dot{\varphi}_0}{\ell_s}\dot{q}_1 \quad . \tag{79}$$

The characteristic exponents of this system of equations are

$$\lambda = \pm i\sqrt{\frac{k}{M} + 3\dot{\varphi}_0^2}\ , 0, 0 \quad .$$

This implies that the frequency of oscillation is $\sqrt{k/M + 3\dot{\varphi}_0^2}$ which is the same as that found for the gravity gradient stabilized case. The repeated zero roots imply that a constant and a term having a linear growth in time are also solutions to the linear system of equations. However, equation (77) gives us the fact that angular momentum is conserved, or that

$$\ell^2\dot{\varphi} = \text{const.} = H \quad .$$

Putting

$$\dot{\varphi}^2 = \frac{H^2}{\ell^4} \tag{80}$$

into equation (76) yields

$$\ddot{\ell} = \frac{H^2}{\ell^3} - \frac{k}{M}(\ell - \ell_0)$$

which, after linearization, yields

$$(81) \qquad \ddot{q}_1 = -\left[\frac{k}{M} + 3\frac{H^2}{\ell_s^4}\right] q_1 = -\left[\frac{k}{M} + 3\dot{\varphi}_0^2\right] q_1 = -\beta q_1$$

where

$$\beta = \left[\frac{k}{M} + 3\dot{\varphi}_0^2\right] \quad .$$

The characteristic exponents of (81) are easily seen to be $\pm\sqrt{k/M + 3\dot{\varphi}_0^2}$. After linearizing equation (80), we get

$$\dot{q}_2 = -\frac{2\dot{\varphi}_0}{\ell_s} q_1$$

or

$$(82) \qquad q_2 = -\frac{2\dot{\varphi}_0}{\ell_s}\left[-\frac{A}{\beta}\cos\beta t + \frac{B}{\beta}\sin\beta t\right] + C$$

where A, B and C are constants determined by initial conditions. From (82) it is easy to see that the solutions for q_1 and q_2 are in fact neutrally stable and that the instability indicated by the repeated zero roots is a consequence of not conserving angular momentum. If the class of solutions is properly restricted, the solutions are all neutrally

stable. The importance of this "trivial instability" will be shown in what follows for the system where R is finite.

When R is finite, the equations can be linearized around the same free space motion as before, but now, this motion does not represent a stationary point. After linearizing about

$$\ell_s = \frac{\frac{k}{M}\ell_0}{\left(\frac{k}{M} - \dot{\varphi}_0^2 - \frac{G}{2R^3}\right)} \quad , \qquad \dot{\varphi}_0 = \text{const.} = \text{reference spin rate}$$

$$\text{and } \varphi_0 = \dot{\varphi}_0 t + \varphi_{\text{initial}}$$

we obtain the spring length deviation

$$(83)\quad \ddot{q}_1 = -\left[\left(\frac{k}{M} - \dot{\varphi}_0^2 - \frac{G}{2R^3}\right) - \frac{3G}{2R^3}\cos 2(\varphi_0 - \theta)\right] q_1 + 2\dot{\varphi}_0 \ell_s \dot{q}_2$$

$$- \frac{3G\ell_s}{R^3}\sin 2(\varphi_0 - \theta) q_2 + \frac{3G\ell_s}{2R^3}\cos 2(\varphi_0 - \theta)$$

and the angular deviation

$$(84)\quad \ddot{q}_2 = -\left[\frac{3G}{R^3}\cos 2(\varphi_0 - \theta)\right] q_2 - \frac{2\dot{\varphi}_0}{\ell_s}\dot{q}_1 - \frac{3G}{2R^3}\sin 2(\varphi_0 - \theta) \quad .$$

These two equations are valid for any orbit and spin rate. To this point, the two changes in the original nonlinear, exact equations (45) through (48) are: (a) an expansion in ℓ/R and keeping of first order terms, and (b) linearization of this expanded set about the free space motion where $R = \infty$. These equations, (83) and (84), constitute a linear, homogeneous, coupled set of ordinary differential equations with time dependent coefficients.

There are basically two such coefficients: (1) G/R^3 and (2) cosine and sine of $2(\varphi_0 - \theta)$. In general, these two types of terms are periodic but do not have the same or commensurate periods. There is no general stability theory that applies to a system of equations such as (83) and (84). The interesting special cases that can be treated analytically have already been shown. However, the case where the two types of terms have commensurate periods can be treated using Floquet stability theory[9] and a numerical integration of the equations.

5. Floquet Theory

Equations (83) and (84) can be transformed into four first order equations by the introduction of two new variables

$$\dot{q}_1 = p_1 \quad \text{and} \quad \dot{q}_2 = p_2 \quad .$$

This yields a system of equations whose general form is

$$\{\dot{q}\} = [A(t)]\{q\} + \{b(t)\} \tag{85}$$

where $[A(t)]$ is the square nxn matrix of coefficients, $\{b(t)\}$ is the 1xn column matrix of forcing functions, and $\{q\}$ is the 1xn column matrix of dependent variables.

If $[A(t)]$ has only constant elements, system (85) can be treated by standard methods such as described in Chapter 6 of Reference 13. However, this is not the case for the dumbbell spinning in orbit. If $[A(t)]$ is periodic, and its largest period is commensurate with the largest period of $\{b(t)\}$, Floquet theory may be applied to system (85). To put (85) into the proper form, we introduce an artificial variable, Z, such that

$\dot{Z} \equiv 0$ which yields a homogeneous set, namely

$$\begin{Bmatrix} \dot{q}_1 \\ \vdots \\ \dot{q}_n \\ \dot{Z} \end{Bmatrix} = \left[\begin{array}{c|c} [A(t)] & \{b(t)\} \\ \hline [0] & 0 \end{array}\right] \begin{Bmatrix} q_1 \\ \vdots \\ q_n \\ Z \end{Bmatrix}$$

or

$$\{\dot{q}\} = [A'(t)]\{q\} \quad . \tag{86}$$

The matrix $[A'(t)]$ is periodic if

$$[A'(t + \tau)] = [A'(t)] \qquad t \geq 0$$

for some period $\tau \geq 0$. A matrix $[F(t)]$ whose columns are linearly independent solutions of (86) is called a fundamental matrix. Thus, $[F(t)]$ satisfies (86). Also, if $[F(t)]$ is a fundamental matrix, so is $[F(t + \tau)]$ and there exists a nonsingular matrix, $[M]$, sometimes called the monodromy matrix[14], such that

$$[F(t + \tau)] = [F(t)][M] \quad . \tag{87}$$

$[M]$ may be reduced to its Jordan normal form and the eigenvalues, $\lambda_1, \ldots, \lambda_n$ are called multipliers. None of the multipliers vanish since

$$\lambda_1\lambda_2 \cdots \lambda_n = \det[M] = \exp \int_0^\tau \text{trace } [A(t)]\, dt \neq 0.$$

In fact, since the trace of $[A(t)] \neq 0$ for most cases (i.e. $\sum_{i=1}^{m} a_{ii}(t) \not\equiv 0$), we conclude that

$$\det [M] = \lambda_1 \lambda_2 \cdots \lambda_n = 1.$$

The trace of $[A(t)]$ being zero means that the acceleration, $\ddot{q}_i$, does not depend on the velocity, $\dot{q}_i$. This is true of any spring mass system in orbit as long as no velocity dependent damping is present. If for example, viscous damping is present, the trace of $[A(t)]$ would be a negative constant and the product of the λ's would be less than one. As will be shown later, this means that the system for most cases is asymptotically stable. Stated physically, this means the system cannot continue to oscillate if damping is present, unless it is forced.

Let us now consider how to obtain the matrix [M] and the multipliers. If we take $t = 0$ and let

$$[F(0)] = [I] \tag{88}$$

where [I] is the identity matrix, we see that

$$[M] = [F(\tau)] \quad . \tag{89}$$

We can obtain $[F(\tau)]$ by numerically integrating system (86) $n + 1$ times for the various initial conditions which yield equation (88). That is

$$\begin{Bmatrix} q_1(0) \\ q_2(0) \\ \vdots \\ z(0) \end{Bmatrix} = \begin{Bmatrix} 1 \\ 0 \\ 0 \\ \vdots \\ 0 \end{Bmatrix}, \begin{Bmatrix} q_1(0) \\ q_2(0) \\ \vdots \\ z(0) \end{Bmatrix} = \begin{Bmatrix} 0 \\ 1 \\ \vdots \\ 0 \end{Bmatrix}, \ldots, \begin{Bmatrix} q_1(0) \\ q_2(0) \\ \vdots \\ z(0) \end{Bmatrix} = \begin{Bmatrix} 0 \\ 0 \\ \vdots \\ 1 \end{Bmatrix} \quad .$$

This amounts to integrating the homogeneous part of the original nonnomogeneous set, (85), for various initial conditions and, lastly, integrating the nonhomogeneous set with zero initial conditions (remember that Z = 1, but Z is only an articificial variable). The system of equations is integrated over period τ each time and the monodromy matrix is formed as in (89). The form of [M] is general except for its last column where [M] is given as

$$[M] = \left[\begin{array}{c:c} \underset{(n \times n+1)}{[M']} & \begin{Bmatrix} 0 \\ 0 \\ \vdots \\ 0 \\ 1 \end{Bmatrix} \end{array}\right] . \tag{90}$$

The last column is the variable Z which is a constant and, hence, must retain its initial value throughout any given solution. From the form of (90), it is easy to see that $\lambda = 1$ must be an eigenvalue for any forced set.

Let us now examine the stability implied by various λ's. We first assume [M] to have n + 1 linearly independent vectors or, stated another way, that the Jordan normal form of [M] is diagonal. By a similarity transformation of (87), we can get

$$[C][F(t+\tau)][C]^{-1} = [C][F(t)][C]^{-1}[C][M][C]^{-1}$$

and defining $[F'(t+\tau)] = [C][F(t+\tau)][C]^{-1}$

and $[J] = [C][M][C]^{-1}$

we get $[F'(t+\tau)] = [F'(t)][J]$

where [J] is the Jordan normal form of [M] and [F'(t)] is still a fundamental matrix of system (86). If the columns of [F'(t)] are written as the linearly independent solutions, we get, in general,

$$\{q_i(t+\tau)\} = \lambda_i \{q_i(t)\} \qquad i = 1, 2, \ldots, n+1 \; . \tag{91}$$

From this, we can see that during the time interval t to $t + \tau$ the magnitude of the vector decreases, remains constant or increases according to $|\lambda_i|$. This is the stability criterion sought.

An interesting case results when the monodromy matrix is not reducible to a diagonal Jordan form. When this happens, it means that at least one λ is repeated at least once and that there are not $n + 1$ linearly independent vectors associated with the monodromy matrix. If the repeated roots are not of unit magnitude, this has no bearing on the stability question. However, if they are equal to 1.0, it represents a polynomial growth with time. The order of the polynomial is one less than the order of the corresponding diagonal block matrix in the Jordan matrix. In summary,

$|\lambda_i| > 1.0$ exponentially unstable

$|\lambda_i| < 1.0$ exponentially stable

$|\lambda_i| = 1.0$ (not repeated) neutrally stable

$|\lambda_i| = 1.0$ (repeated) either neutrally stable or polynomial growth with time depending on [J].

To point out the application of the theory, let us examine a well-known equation which can be handled analytically, namely, the equation for the forced harmonic oscillator

(92) $$\ddot{X}(t) + \omega_0^2 X(t) = \cos \omega t.$$

By defining $\dot{X} = Y$, we can put (92) into the form of (86).

$$\begin{Bmatrix} \dot{Y} \\ \dot{X} \\ \dot{Z} \end{Bmatrix} = \begin{bmatrix} 0 & -\omega_0^2 & \cos \omega t \\ 1 & 0 & 0 \\ 0 & 0 & 0 \end{bmatrix} \begin{Bmatrix} Y \\ X \\ Z \end{Bmatrix}$$

The column vectors of initial conditions to form the identity matrix are

$$\begin{Bmatrix} 1 \\ 0 \\ 0 \end{Bmatrix}, \quad \begin{Bmatrix} 0 \\ 1 \\ 0 \end{Bmatrix}, \quad \begin{Bmatrix} 0 \\ 0 \\ 1 \end{Bmatrix} .$$

In this case, the period $\tau = 2\pi/\omega$. Since the solution to equation (92) is known, we can form the monodromy matrix. Let $\omega_0^2 = \pi^2$ and $\omega = 2\pi$ for simplicity. We get

(93) $$[M] = \begin{bmatrix} -1 & 0 & \frac{2}{3\pi^2} \\ 0 & -1 & 0 \\ 0 & 0 & 1 \end{bmatrix}$$

The characteristic equation is

$$(1 + \lambda)(1 + \lambda)(1 - \lambda) = 0 \qquad \therefore \qquad \lambda = -1, -1, 1.$$

The roots are repeated and the solution may or may not be stable. Now, instead of finding [J] for (93), which for arbitrary matrices may be difficult to do directly, we determine the rank of the matrix

$$(94) \qquad \left[[M] - (-1)[I]\right] = \begin{bmatrix} 0 & 0 & \frac{2}{3\pi^2} \\ 0 & 0 & 0 \\ 0 & 0 & 0 \end{bmatrix}$$

from which we can find the nullity of [M] (i.e., (nullity) = (order) − (rank)). The (multiplicity)−(nullity) of the repeated root gives us the number of off diagonal entries for the Jordan normal form of the matrix [M]. The rank is defined as the order of the largest nonvanishing subdeterminant. In this case, the rank is unity because all determinants of order two and three are obviously zero. Thus, the nullity is equal to the multiplicity and the Jordan form has no off diagonal terms and the system is neutrally stable.

Now for the case for $\omega_0 = \omega$, which we know to be unstable, the monodromy matrix is

$$(95) \qquad [M] = \begin{bmatrix} 1 & 0 & 0 \\ 0 & 1 & 1/2 \\ 0 & 0 & 1 \end{bmatrix} .$$

The characteristic equation is

$$(1 - \lambda)(1 - \lambda)(1 - \lambda) = 0 \qquad \therefore \qquad \lambda = 1, 1, 1.$$

Again the roots are repeated but now the multiplicity is three and the nullity of

$$\left[[M] - (1)[I]\right] = \begin{bmatrix} 0 & 0 & 0 \\ 0 & 0 & 1/2 \\ 0 & 0 & 0 \end{bmatrix}$$

is obviously again two, so that the (multiplicity)–(nullity) is one and the Jordan form of (95) has one off diagonal term. This represents a linear growth with time of one of the solutions.

Note that the trace of the coefficient matrix for (92) is zero which implies that the product, $\lambda_1\lambda_2\lambda_3 = 1.0$ as it must be. As previously mentioned, the artificial variable Z introduces a predetermined λ equal to 1.0. Periodic forcing functions in a system of linear equations can only add particular solutions having, at most, a polynomial growth with time and never an exponential growth or decay.

One more example will be shown to point out the effect of viscous damping which was mentioned at the early part of the discussion of Floquet theory. Given the damped equation

$$\ddot{X} + C\dot{X} + X = 0$$

where a forcing term has been omitted at no loss of generality, and defining $\dot{X} = Y$, we get

$$\begin{Bmatrix} \dot{X} \\ \dot{Y} \end{Bmatrix} = \begin{bmatrix} 0 & 1 \\ -1 & -C \end{bmatrix} \begin{Bmatrix} X \\ Y \end{Bmatrix} . \tag{96}$$

Here the trace of the coefficient matrix is $(-C)$, and, thus, we know

$$\lambda_1\lambda_2 = \exp \int_0^\tau (-C)dt = e^{-C\tau} .$$

Since [A(t)] in (96) is a constant matrix, any positive, nonzero, finite number can be thought of as the period of the matrix. The monodromy matrix for C = 2 and $\tau = 1$ is

$$[M] = \begin{bmatrix} 2e^{-1} & e^{-1} \\ -e^{-1} & 0 \end{bmatrix}$$

and the characteristic equation is

$$\lambda^2 - 2e^{-1}\lambda + e^{-2} = 0 \quad .$$

Thus the roots are

$$\lambda = e^{-1}, e^{-1}$$

hence

$$\lambda_1\lambda_2 = e^{-2} = e^{-C\tau} \quad \text{since} \quad C = 2, \tau = 1.$$

Here the λ's are less than 1.0 in magnitude and, therefore, represent a decay or asymptotic stability. Had C been a negative number, an asymptotic instability would exist. The effect of the forcing term must be examined only when one of the roots of the homogeneous set has a multiplier of 1.0. Unfortunately, this is the case for the dumbbell spinning in the gravity gradient.

6. Application of Floquet Theory

Strictly speaking, Floquet theory applies only to a periodic coefficient matrix, [A(t)]. However, [A(t)] can be considered to be

periodic, even if it is not, to within a given accuracy if its elements are all periodic and if one chooses a period for [A(t)] which is sufficiently long so that periodicity is approximated. The practical limit on the usefulness of this fact is usually computer accuracy. The more points the computer must take to integrate over the given period, the lower the accuracy of the end result. Hence, if an extremely long time interval must be taken to adequately approximate periodicity of [A(t)], the accuracy of the integration will be in question due to round-off errors.

The Floquet stability theory described in the previous section was applied to equations (83) and (84) for circular orbits where the one time variant coefficient, G/R^3, was constant. The equations are forced, so one must watch for repeated roots of the homogeneous equations set equal to 1. In all the cases examined, two multipliers having this value were found in addition to the one from the artificial variable, Z. Because the nullity was always two and the nultiplicity was three, a linear growth with time was indicated.

However, recall that a linear growth in time was also found for the system in free space when angular momentum of the reference motion was not preserved by the initial conditions. This was identified as a "trivial instability" and merely indicated that the position angle was deviating from the reference angle, linearly with time, but that the spin rate was not growing. The remaining multipliers had a magnitude of 1.0 but were not repeated; hence, they represented neutral stability or periodic motion for the cases considered. Since the motion given by the linearized equations is periodic, the validity of the linearization is open to question.

When neutral stability of the linearized equations is found for a nonlinear system, no conclusions can be stated concerning the stability of the nonlinear system. In this case, one must actually integrate the nonlinear equations numerically and observe the motion. On the other hand, if exponential stability or instability is indicated for the linearized equations, the the nonlinear system is also stable or unstable respectively.

The expanded nonlinear system of equations (61) through (62) were numerically integrated and this motion compared to the motion calculated using the linearized system (83) and (84). The agreement was surprisingly good as can be seen from Figures 7, 8, and 9 for circular orbits. Figure 7 shows the axial stretching or deviation of the subsatellite due to the gravity gradient for various orbits and spring stiffnesses. The shape of the curve and its dependence on orbital radius suggested the following empirical formula for the gravity gradient perturbation in length.

$$\Delta \ell = 115 \left(\frac{G}{R^3}\right) \frac{\ell_0}{\left(\frac{k}{M} - \dot{\varphi}_0^2 - \frac{G}{2R^3}\right)} \quad .$$

This equation has been verified only by comparison with Figure 7, and its validity for spin rates other than one revolution per hour has not been demonstrated. The effective spring constants plotted correspond roughly to a 20 mils x 6 miles, nylon cable attached to a 100 pound subsatellite.

Figure 8 shows that the spin rate deviation from the nominal rate of one rev./hour is considerably less than $\pm$ 1% for orbits above 14,000 nautical miles. Figure 9 is the transverse deviation of a subsatellite due to gravity effects. The curve shows that the oscillations are quite small when compared to the size of the overall system.

Floquet theory was also applied to certain cases of elliptic orbits, with and without damping. For the cases where the periodic coefficients were commensurate, the theory showed that the system was either neutrally stable as before or asymptotically stable when damping was included. The only instability found in all the cases examined, occurred when the system was spinning in an orbit which was low enough to drastically and permanently change the spin rate.

An example of this is shown in Figure 10, which depicts the effect of an extremely low perigee. According to Floquet theory the system is unstable and a subsequent numerical integration of the nonlinear equations confirmed this. Note that the spin rate can be either increased or decreased during perigee passing depending on its orientation prior to reaching perigee. If the perigee is increased to 10,000 nautical miles for the same apogee, the system becomes stable. Figure 11 demonstrates this. The oscillations in spin rate change as $1/R^3$ as the system proceeds around the orbit but no net change is experienced. The linear growth in the angular position shown in Figure 11 is the so called "trivial" instability" previously discussed.

In summary, the subsatellite wire system, neglecting the transverse motion of the wire, appears to be neutrally stable in circular and certain elliptic orbits for spin rates of one and ten rev./hour. The linearized analysis has been shown to be useful and, indeed, predicts an instability for low orbits. The next chapter deals with the dynamics of the connecting wire using the lumped mass approach.

CHAPTER IV

DYNAMICS OF A SPINNING RADIAL WIRE

The motion of a mass connected to a much heavier mass in orbit has been shown to be stable for many cases. The next step is to examine the motion of the connecting wire when it is not assumed to be massless. Assumptions such as uncoupling of radial and transverse motion and also constant tension have been made by previous authors to enable solutions to be obtained.

The approach here is to consider a lumped mass system and treat the ordinary differential equations without assuming the tension to be constant and without neglecting Coriolis effects. To study the line dynamics, the equations of motion for the three mass model shown in Figure 2 were derived previously in general form as equations (38) and (39). When three masses are considered, these equations become

$$(97)\quad \ddot{\ell}_1 = \ell_1\dot{\varphi}_1^2 - \frac{G\ell_1}{R^3}\left[1 - 3\cos^2(\varphi_1 - \theta)\right] - \frac{k_1}{M_1}(\ell_1 - \ell_{10}) - \frac{k_2}{M_1}\left\{1 - \frac{\ell_{20}}{e_2}\right\}\left[\ell_1 - \ell_2\cos(\varphi_1 - \varphi_2)\right]$$

$$(98)\quad \ddot{\varphi}_1 = -\frac{2\dot{\ell}_1\dot{\varphi}_1}{\ell_1} - \frac{3G}{2R^3}\sin 2(\varphi_1 - \theta) - \frac{k_2}{M_1}\left\{1 - \frac{\ell_{20}}{e_2}\right\}\frac{\ell_2}{\ell_1}\sin(\varphi_1 - \varphi_2)$$

$$(99)\quad \ddot{\ell}_2 = \ell_2\dot{\varphi}_2^2 - \frac{G\ell_2}{R^3}\left[1 - 3\cos^2(\varphi_2 - \theta)\right]$$

$$- \frac{k_2}{M_2}\left\{1 - \frac{\ell_{20}}{e_2}\right\}\left[\ell_2 - \ell_1\cos(\varphi_1 - \varphi_2)\right]$$

$$- \frac{k_3}{M_2}\left\{1 - \frac{\ell_{30}}{e_3}\right\}\left[\ell_2 - \ell_3\cos(\varphi_2 - \varphi_3)\right]$$

$$(100)\quad \ddot{\varphi}_2 = -\frac{2\dot{\ell}_2\dot{\varphi}_2}{\ell_2} - \frac{3G}{2R^3}\sin 2(\varphi_2 - \theta) + \frac{k_2}{M_2}\left\{1 - \frac{\ell_{20}}{e_2}\right\}\frac{\ell_1}{\ell_2}\sin(\varphi_1 - \varphi_2)$$

$$- \frac{k_3}{M_2}\left\{1 - \frac{\ell_{30}}{e_3}\right\}\frac{\ell_3}{\ell_2}\sin(\varphi_2 - \varphi_3)$$

$$(101)\quad \ddot{\ell}_3 = \ell_3\dot{\varphi}_3^2 - \frac{G\ell_3}{R^3}\left[1 - 3\cos^2(\varphi_3 - \theta)\right]$$

$$- \frac{k_3}{M_3}\left\{1 - \frac{\ell_{30}}{e_3}\right\}\left[\ell_3 - \ell_2\cos(\varphi_2 - \varphi_3)\right]$$

and finally

$$(102)\quad \ddot{\varphi}_3 = -\frac{2\dot{\ell}_3\dot{\varphi}_3}{\ell_3} - \frac{3G}{2R^3}\sin 2(\varphi_3 - \theta) + \frac{k_3}{M_3}\left\{1 - \frac{\ell_{30}}{e_3}\right\}\frac{\ell_2}{\ell_3}\sin(\varphi_2 - \varphi_3).$$

The terms in equations (97) through (102) may be identified as follows: On the right-hand side, the first term is the Coriolis force, the second term is the gravity force and the third, and in some equations the fourth term, is the elastic or spring force. The above equations are valid for

any orbit, spin rate and deflections. In particular, the assumption of small deflections has not been made.

To determine whether the two masses representing the continuous cable are sufficient to determine its motion, the frequencies of the continuous nonrotating cable with constant tension were compared with those for the linearized, nonrotating lumped model. To do this, the three mass model must be altered to that of Figure 12. In this model, both ends are fixed and the masses have only one degree of freedom each, namely, Y_1 and Y_2. This analysis will yield a fourth order coefficient matrix whose roots will give the two natural frequencies of the system.

The kinetic energy is given by

$$T = \frac{M_1}{2} \dot{Y}_1^2 + \frac{M_2}{2} \dot{Y}_2^2$$

and the potential energy, keeping up to fourth order terms in Y_1, Y_2, is

$$V = 1/2\ k_1 \left[L_0 - L - 1/2\ \frac{Y_1^2}{L} \right] + 1/2\ k_2 \left[L_0 - L - 1/2\ \frac{(Y_2 - Y_1)^2}{L} \right]^2$$

$$+ 1/2\ k_3 \left[L_0 - L - 1/2\ \frac{Y_2^2}{L} \right]$$

where L_0 and L are respectively the unstretched and stretched spring lengths. The linear equations of motion which result after again dropping higher order terms are

$$(103) \qquad \ddot{Y}_1 = \left(\frac{k_1}{M_1} + \frac{k_2}{M_1} \right) \left(\frac{L_0}{L} - 1 \right) Y_1 - \frac{k_2}{M_1} \left(\frac{L_0}{L} - 1 \right) Y_2$$

and

$$\ddot{Y}_2 = -\frac{k_2}{M_2}\left(\frac{L_0}{L} - 1\right) Y_1 + \left(\frac{k_2}{M_2} + \frac{k_3}{M_2}\right)\left(\frac{L_0}{L} - 1\right) Y_2 \quad . \tag{104}$$

For a cable with constant geometric and elastic properties along its length (i.e. $k_1 = k_2 = k_3$ and $M_1 = M_2$), we define a constant H as

$$H = \frac{k}{M}\left(1 - \frac{L_0}{L}\right) \quad .$$

Thus the coefficient matrix of the equivalent first order system is

$$[A] = \begin{bmatrix} 0 & 0 & 1 & 0 \\ 0 & 0 & 0 & 1 \\ -2H & H & 0 & 0 \\ H & -2H & 0 & 0 \end{bmatrix} \quad .$$

The characteristic equation is

$$\lambda^4 + 4H\lambda^2 + 3H^2 = 0$$

with roots

$$\lambda = \pm i\sqrt{H} \ , \ \pm i\sqrt{3H} \tag{106}$$

which are the first and second natural frequencies respectively. These frequencies are to be compared with those of an equivalent continuously distributed mass cable. The frequencies for a continuous cable are well known and are given by

$$\alpha = \sqrt{\frac{T}{\rho}}\frac{\pi}{L'}\ ,\ 2\sqrt{\frac{T}{\rho}}\frac{\pi}{L'}\ ,\ \ldots,\ n\sqrt{\frac{T}{\rho}}\frac{\pi}{L'}$$

where T = tension, ρ = mass density/unit length and L' = total length of cable. Since

$$H = \frac{k}{M}\left(1 - \frac{L_0}{L}\right) = \frac{1}{LM}\ [k(L - L_0)] = \frac{T}{LM}$$

we can take the ratio of the two lowest frequencies and, noting that $M = \rho L'/3$ and $L = L'/3$, we get

$$\frac{\text{continuous}}{\text{lumped}} = \frac{\pi}{3} \text{ or } \sim 4\ 1/2\ \% \text{ error.}$$

For the second natural frequency, we get

$$\frac{\text{continuous}}{\text{lumped}} = \frac{2\pi}{\sqrt{27}} \text{ or } \sim 17\% \text{ error.}$$

From the above calculations, it can be seen that the first frequency is reasonably accurate while the second is somewhat in error as would be expected for such a crude approximation to a continuous cable.

The next step is to determine the effects of the Coriolis force on the transverse frequencies of a spinning cable. To do this, the single mass model having two degrees of freedom as shown in Figure 13 was used. This simplification was made to keep the coefficient matrix to fourth order so the roots could be easily extracted. The overall spin rate was fixed. This case would correspond to a mass which is much heavier than the connecting cable spinning in free space. The kinetic energy is

$$T = \frac{M}{2}\left[\dot{\ell}^2 + \ell^2(\dot{\varphi} + \omega)^2\right]$$

where ω is the given overall spin rate and $\dot{\varphi}$ is the spin rate of the mass point relative to ω. The potential energy is

$$V = \frac{k}{2}\left[(\ell - \ell_0)^2 + \left(\sqrt{\ell^2 + L^2 - 2\ell L\cos\varphi} - \ell_0\right)^2\right]$$

where ℓ = inner spring length, ℓ_0 = unstretched length of both springs and L = overall length of system. The equations of motion after linearization are, in matrix form

$$(107)\begin{Bmatrix} \dot{q}_1 \\ \dot{q}_2 \\ \dot{p}_1 \\ \dot{p}_2 \end{Bmatrix} = \begin{bmatrix} 0 & 0 & 1 & 0 \\ 0 & 0 & 0 & 1 \\ \left(\omega^2 - \frac{2k}{M}\right) & 0 & 0 & L\omega \\ 0 & -\frac{2k}{LM}(L - 2\ell_0) & -\frac{4\omega}{L} & 0 \end{bmatrix}\begin{Bmatrix} q_1 \\ q_2 \\ p_1 \\ p_2 \end{Bmatrix}$$

The natural frequencies are

$$(108)\ \lambda = \pm i\sqrt{\frac{3\omega^2}{2} + \frac{2k}{M}\left(1 - \frac{\ell_0}{L}\right) \pm \sqrt{\omega^2\left(\frac{9\omega^2}{4} + \frac{8k}{M} - \frac{10k\ell_0}{ML}\right) + 4\left(\frac{k\ell_0}{ML}\right)^2}}\ .$$

We can check this result at $\omega = 0$ to see how well the one mass approximation agrees with the continuous cable in the same way as before. We get

$$\frac{\text{continuous}}{\text{lumped}} = \frac{\pi}{\sqrt{8}} \text{ or } \sim 7\% \text{ error.}$$

If equation (108) is expanded in terms of ω^2 and only first order terms are retained, we get

$$\lambda = \pm i \sqrt{\frac{2k}{M}\left(1 - \frac{2\ell_0}{L}\right) - 4\omega^2\left(\frac{L}{2\ell_0} - 1\right)} \tag{109}$$

and

$$\lambda = \pm i \sqrt{\frac{2k}{M} + \omega^2\left(\frac{2L}{\ell_0} - 1\right)} \quad . \tag{110}$$

From equation (109) the effect of spinning at a constant rate and under constant tension, is to lower the frequency associated with the transverse mode. Equation (110), for $\omega = 0$, corresponds to the axial mode and the effect of spinning is to increase that frequency. This is the same effect that was found for the axial frequency for the single mass, namely a stiffening effect due to rotation. For $\omega = 0$, the axial and transverse modes are uncoupled in the linear equations but when the system is spinning, they are coupled by linear terms through the Coriolis effect. Thus when speaking of the "axial" or "transverse" frequency of a spinning system, one usually means the frequency of the motion which is predominantly in the axial or transverse direction even though the two motions are coupled. The above conclusions are the same as those reached for the distributed mass cable in Chapter II.

To examine the effects of large deflections, the system of equations (97) through (102) was numerically integrated for varying tension and initial amplitude with $R \cong \infty$ (i.e., free space) and mass three restrained at a constant radius but free in the tangential direction. These numerical results for both spinning and nonspinning cases compared favorably with the frequencies calculated for the various simplified models above.

A plot of amplitude versus frequency for two specific cases can be seen in Figure 14.

When the end mass is unrestrained and the lowest transverse frequency is equal to or near to the axial frequency, a parametric type motion can occur. This motion is not the type of parametric motion usually found because the two modes affected are directly coupled through their linear terms. When the axial mode is excited, the Coriolis effects directly exert a transverse force on each mass point of the cable. The force on each mass point is different because the Coriolis force is a function of the radial velocity and the spin rate. Hence the magnitude of the Coriolis acceleration varies along the cable. Since the outer mass is much heavier, its acceleration and corresponding displacement are smaller than those for the lighter mass points of the cable. This causes transverse deflections to result due to the axial motion of the cable. It is this phenomenon which may cause large deflections in a spinning system.

The gravity forces on each mass point can be seen to be independent of its radius from the center of rotations for the linear approximation and, therefore, can not easily start transverse motions of the cable. To show this, we define a nondimensional variable as

$$M_1(t) = \frac{q_1(t)}{\ell_s}$$

and introduce this into equations (83) through (84). Thus the equations are independent of the steady state length, namely

$$(111)\quad \ddot{M}_1 = -\left[\left(\frac{k}{M} - \dot{\varphi}_0^2 - \frac{G}{2R^3}\right) - \frac{3G}{2R^3}\cos 2(\varphi_0 - \theta)\right] M_1 + 2\dot{\varphi}_0 \dot{q}_2$$

$$-\left[\frac{3G}{R^3}\sin 2(\varphi_0 - \theta)\right] q_2 + \frac{3G}{2R^3}\cos 2(\varphi_0 - \theta)$$

and

$$(112)\quad \ddot{q}_2 = -\left[\frac{3G}{R^3}\cos 2(\varphi_0 - \theta)\right] q_2 - 2\dot{\varphi}_0 \dot{M}_1 - \frac{3G}{2R^3}\sin 2(\varphi_0 - \theta).$$

This implies that an inelastic string, which was initially straight and spinning in the gravity gradient, would remain straight according to the linearized equations because the gravity gradient would cause all masses to speed up and slow down at the same rate. However, elastic stretching due to the gravity gradient and the resulting Coriolis acceleration cause oscillations and, as is the case in most elastic systems, the frequencies of the axial and transverse motions must not be in resonance or large deflections will result. Figure 15 shows a case where the transverse oscillations developed with time while Figure 16 shows the beating phenomenon when the transverse oscillations were started initially.

1. Damping Effects

Damping is usually regarded as a "cure all" for most dynamics problems. The damping terms have already been derived—equations (41) and (42). Let us now linearize these terms about a straight line configuration to determine the effect of damping for small oscillations. They become

$$-\frac{C_j}{M_j}\dot{e}_j \cos\alpha_j - \frac{C_{j+1}}{M_j}\dot{e}_{j+1}\cos\epsilon_j =$$

$$-\frac{C_j}{M_j}\left[\dot{q}_j - 1\ell(j-1)_0 + \dot{q}_j\,\ell j_0 - \left[\dot{q}_j - 1\ell j_0 + \dot{q}_j\ell(j-1)_0\right]\right]$$

$$-\frac{C_{j+1}}{M_j}\left[\dot{q}_j\ell j_0 + \dot{q}_{j+1}\ell(j+1)_0 - \left[\dot{q}_j\ell(j+1) + \dot{q}_{j+1}\ell j_0\right]\right] + \mathcal{O}(q)^2$$

and

$$-\frac{C_j}{M_j}\frac{\dot{e}_j \sin\alpha_j}{\ell_j} - \frac{C_{j+1}}{M_j}\frac{\dot{e}_{j+1}\sin\epsilon_j}{\ell_j} = 0 + \mathcal{O}(q)^2$$

where q_j's are the deviations in the lengths ℓ_{i_0}. Note that the angular deviations p_j, do not enter into the linear damping terms.

This implies there is no direct damping in these coordinates for small deflections. This can be shown by comparing Figure 17 with Figure 18. The first case has no damping and the oscillations continue with a slight beat amplitude. In the second case, the axial oscillation is effectively damped in several oscillations and the transverse oscillations are reduced in amplitude initially, but continue to oscillate long after the axial motion has damped out. This indicates that damping cannot be relied upon to significantly reduce transverse line motion for small deflections (small in a mathematical sense and not necessarily small in a physical sense) as previous papers such as the one by Targoff have suggested.

It is not anticipated that the small amount of flexural damping which would be present in a physical system, will effectively damp out the lower modes due to the small radii of curvature of the long thin

connecting cable. Deflections of a hundred feet for a 16,000 foot cable produce negligible bending and the cable's flexural damping coefficient will also be quite small. Builders of these systems will have to accept a certain degree of motion unless special dampers which will effectively damp the transverse motion are designed.

2. Motion of the Radial Wire out of the Orbital Plane

All the analysis to this point has allowed only motions in the plane of the orbit. This is certainly a large class of problems. However, it remains to be shown that this motion can be examined independently of the other possibilities. It can be argued that a single mass on the end of a massless spring spinning in the orbital plane will experience no forces perpendicular to the orbital plane. The Coriolis, elastic, centrifugal and gravity forces all act in the plane.

The same is true for the connecting cable; however, small perturbations may occur to disturb it out of the orbital plane even though the heavier subsatellite remains essentially in the plane. This chapter examines this problem for out of plane motion of the cable mass points, but plane motion of the subsatellite.

Figure 19 shows the coordinate system used to define the position of each mass. The important quantities needed to derive the new equations are, (1) the length of each spring

$$e_i = \sqrt{\ell_i^2 + \ell_{i-1}^2 - 2\ell_{i-1}\ell_i(\cos\psi_{i-1}\cos\psi_i\cos(\varphi_i - \varphi_{i-1}) + \sin\psi_{i-1}\sin\psi_i)}$$

and (2) the distance from the Earth's center to the i^{th} mass

$$|\bar{r}_i| = \sqrt{R^2 + \ell_i^2 + 2R\ell_i \cos\psi_i \cos(\varphi_i - \theta)} \quad .$$

The Lagrange equations of motion are

$$\ddot{\ell}_j = \ell_j[\cos^2\psi_j\dot{\varphi}_j^2 + \dot{\psi}_j^2] - \frac{k_j}{M_j}\left[1 - \frac{\ell_{j0}}{e_j}\right][\ell_j - \ell_{j-1}(\cos\psi_{j-1} \times$$

$$\times \cos\psi_j \cos(\varphi_j - \varphi_{j-1}) + \sin\psi_j \sin\psi_{j-1})]$$

$$- \frac{k_{j+1}}{M_j}\left[1 - \frac{\ell_{(j+1)0}}{e_{j+1}}\right][\ell_j - \ell_{j+1}(\cos\psi_j \cos\psi_{j+1} \cos(\varphi_{j+1}$$

$$- \varphi_j) + \sin\psi_{j+1} \sin\psi_j)] - \frac{G\ell_j}{R^3}[1 - 3\cos^2\psi_j \cos^2(\varphi_j - \theta)]$$

$$\ddot{\varphi}_j = -\frac{2[\dot{\ell}_j\ell_j\cos^2\psi_j - \ell_j^2\dot{\psi}_j\frac{\sin 2\psi_j}{2}]\dot{\varphi}_j^2}{\ell_j^2\cos^2\psi_j} - \frac{k_j}{M_j}\left[1 - \frac{\ell_{j0}}{e_j}\right] \times$$

$$\times \frac{\ell_{j-1}\cos\psi_{j-1}\sin(\varphi_j - \varphi_{j-1})}{\ell_j\cos\psi_j}$$

$$+ \frac{k_{j+1}}{M_j}\left[1 - \frac{\ell_{(j+1)0}}{e_{j+1}}\right]\frac{\ell_{j+1}\cos\psi_{j+1}\sin(\varphi_{j+1} - \varphi_j)}{\ell_j\cos\psi_j}$$

$$- \frac{3G}{R^3}\sin 2(\varphi_j - \theta)$$

and

$$\ddot{\psi}_j = -\frac{2\dot{\ell}_j\dot{\psi}_j}{\ell_j} - \sin 2\psi_j\dot{\varphi}_j^2$$

$$-\frac{k_j}{M_j}\left[1 - \frac{\ell_{j0}}{e_j}\right]\frac{\ell_{j-1}}{\ell_j}\left[\cos\psi_{j-1}\sin\psi_j\cos(\varphi_j - \varphi_{j-1})\right.$$

$$\left. - \cos\psi_j\sin\psi_{j-1}\right]$$

$$-\frac{k_{j+1}}{M_j}\left[1 - \frac{\ell_{(j+1)_0}}{e_{j+1}}\right]\frac{\ell_{j+1}}{\ell_j}\left[\cos\psi_{j+1}\sin\psi_j\cos(\varphi_{j+1} - \varphi_j)\right.$$

$$\left. - \cos\psi_j\sin\psi_{j+1}\right] - \frac{3G}{2R^3}\sin 2\psi_j\cos^2(\varphi_j - \theta).$$

These equations were also numerically integrated for several cases. The motion was found for: (1) not spinning in free space, (2) spinning in free space, and (3) spinning in orbit. The results may be summarized as follows:

(1) The out of plane frequency is unaffected by the rotation. This was expected since the out of plane motion is not coupled through the Coriolis forces.

(2) When the system is spinning, the in plane frequencies are given by

$$\omega_{IN}^2 = \omega^2\left\{(n\pi)^2\frac{M}{\rho\ell} - 1\right\} \qquad \text{page 23}$$

and the out of plane by

$$\omega_{OUT}^2 = \omega^2 (n\pi)^2 \frac{M}{\rho \ell}$$

since the tension is equal to the centrifugal force of the tip mass. Note that they will be essentially equal if $M/\rho\ell \gg 1$. When they are the same, the cable merely vibrates in and out of the plane as shown in Figure 20.

To emphasize the effect of a rotation where the in plane and out of plane frequencies were different, the end mass was held at a fixed distance so that in terms of the tension the two frequencies were given by

$$\omega_{IN} = \frac{(n\pi)^2 T}{\rho \ell^2} - \omega^2$$

and

$$\omega_{OUT} = \frac{(n\pi)^2 T}{\rho \ell^2} \quad .$$

The tension, T, was very low, compared to what it would have been with a large end mass. Figure 21 is a plot of the motion perpendicular to the imaginary line from the center of rotation to the end mass. The frequencies were different and this produced the interesting pattern shown. Initially, the rotation of the cable about the imaginary line through its end points is counter clockwise and moving back and forth from the second to fourth quadrants. However, after the motion has rotated to the first and third quadrants, it suddenly reverses direction and begins a clockwise rotation.

(3) The out of plane motion does not "feed" on the in-plane motion. In other words, the amplitudes of the two motions are essentially constant with time. Thus, the in plane motion may be treated independently since additional freedom out of the orbital plane will not produce an instability in the planar motion.

CHAPTER V

FINITE BODIES

The analysis to this point has considered all bodies to be point masses. It is certainly possible that some physical systems might have instabilities associated with the finite bodies of the system. The connecting cables will not always be attached to the center of mass of each box, and this can cause rotational instabilities of the bodies when the cable vibrational frequencies are in resonance with the rotational frequencies of the various bodies.

The following analysis demonstrates how the previous approach may also be used to analyze a system with a finite body. The system to be considered consists of a cylinder of radius, a, and mass moment of inertia, I, with two massless radial cables connecting it to two point mass subsatellites of mass, m, (see Figure 22). Obviously, the model could be made more general by assuming more mass points and including gravity gradient terms. The length of each spring, r, is given by

$$r = \sqrt{a^2 + \ell^2 - 2a\ell \cos(\gamma - \varphi)}$$

and the radius vector to each subsatellite from the center of the Earth is given by

$$\sqrt{R^2 + \ell^2 \pm 2R\ell \cos(\varphi - \theta)} \quad .$$

The Lagrange equations of motion are

$$\ddot{\ell} = \ell\dot{\varphi}^2 - \frac{k}{M}\left(1 - \frac{r_0}{r}\right)[\ell - a\cos(\gamma - \varphi)]$$

$$- \frac{G}{2}\left\{\frac{\ell + R\cos(\varphi - \theta)}{A} + \frac{\ell - R\cos(\varphi - \theta)}{B}\right\}$$

$$\ddot{\varphi} = -\frac{2\dot{\ell}\dot{\varphi}}{\ell} + \frac{k}{M}\left(1 - \frac{r_0}{r}\right)\frac{a}{\ell}\sin(\gamma - \varphi)$$

$$+ \frac{G}{2\ell}\left\{\frac{R\sin(\varphi - \theta)}{A} - \frac{R\sin(\varphi - \theta)}{B}\right\}$$

where

$$A = [R^2 + \ell^2 + 2R\ell\cos(\varphi - \theta)]^{3/2} \text{ and } B = [R^2 + \ell^2 - 2R\ell\cos(\varphi - \theta)]^{3/2}$$

and

$$\ddot{\gamma} = -\frac{2k}{I}\left(1 - \frac{r_0}{r}\right)a\ell\sin(\gamma - \varphi), \quad r_0 \equiv \text{unstretched spring length}$$

plus the two orbital equations of motion.

These equations can be linearized about a straight configuration where

$$\gamma_0 = \varphi_0, \ \dot{\gamma}_0 = \dot{\varphi}_0, \text{ and } \ell_s = \frac{\frac{k}{M}(r_0 + a)}{\frac{k}{M} - \dot{\varphi}_0^2} .$$

For free space, the equations are for ℓ, φ, and γ respectively,

$$\ddot{q}_1 = -\left(\frac{k}{M} - \dot{\varphi}_0^2\right) q_1 + 2\ell_s \dot{\varphi}_0 \dot{q}_2$$

$$\ddot{q}_2 = -\frac{2\dot{\varphi}_0 \dot{q}_1}{\ell_s} + \frac{k}{M}\left(1 - \frac{(a + r_0)}{\ell_s}\right) \frac{a}{\ell_s - a} (q_3 - q_2)$$

and

$$\ddot{q}_3 = -\frac{2k}{I}\left(1 - \frac{(a + r_0)}{\ell_s}\right) \frac{a\ell_s^2}{(\ell_s - a)} (q_3 - q_2) \quad .$$

The characteristic equation for the above set of equations yields as usual, two zero roots because of the cyclic coordinate and the following additional two roots which are the natural frequencies,

$$(113)\quad \omega_{1,2} = \pm \left[\frac{k}{2M} + 3\dot{\varphi}_0^2 + \left|1 - \frac{(a + r_0)}{\ell_s}\right| \frac{ka}{(\ell_s - a)} \left|\frac{1}{M} + \frac{2\ell_s^2}{I}\right|\right.$$

$$\pm \frac{1}{2}\left[\left[-\frac{k}{M} - 3\dot{\varphi}_0^2 + \left|1 - \frac{(a + r_0)}{\ell_s}\right| \frac{ka}{(\ell_s - a)} \left(\frac{2\ell_s^2}{I} - \frac{1}{M}\right)\right]^2\right.$$

$$\left.\left. - 4\frac{k}{M}\left(1 - \frac{(a + r_0)}{\ell_s}\right) \frac{a}{(\ell_s - a)} \left(\frac{k}{M} - \dot{\varphi}_0^2 - \frac{2k}{I}\left(1 - \frac{(a + r_0)}{\ell_s}\right) \frac{a\ell_s^2}{(\ell_s - a)}\right)\right]^{1/2}\right]^{1/2}$$

If, in the above expression $\varphi_0 \equiv 0$, then $\ell_s = r_0$ and

$$\omega_{1,2} = \pm\sqrt{\frac{k}{M}}\ ,\ 0,\ 0$$

which is just the spring mass frequency. For $\dot{\varphi}_0 \neq 0$, but $a \equiv 0$ we get

$$\omega_{1,2} = \pm\sqrt{\frac{k}{M} + 3\dot{\varphi}_0^2}\ ,\ 0,\ 0$$

which is the spinning spring mass frequency derived earlier. For the general case, the frequencies are given above in equation (113).

Instabilities may occur when the gravity gradient forcing of the end mass is near a natural frequency for the free space motion given above. The forcing of the end mass could result in the growth of the periodic rotational motion of the center body. A complete study of the stability regions for a particular range of parameters and orbits can be carried out using Floquet theory in the manner discussed above.

CHAPTER VI

CONCLUSIONS

The subsatellite-cable system shown in Figure 1 has been analyzed assuming both a distributed mass and a lumped mass description of the connecting cable. In both descriptions, a linear elastic material was assumed.

For the distributed mass case, the complexity of the resulting nonlinear partial differential equations appears to preclude their use for motion and stability studies of the system, except for a few simple cases. In particular, the equations must be linearized and some of the linear coupling terms neglected in order to obtain solutions.

On the other hand, if the system is approximated by lumped point masses connected by linear elastic massless springs, several practical advantages over the distributed mass approach are obtained.

(a) Lagrange's equations of motions may be systematically derived for any general system by considering the elastic and gravity potentials. This can also be carried out for the distributed mass system, but one must deal with the variation of integrals instead of merely taking partial derivatives, as is the case for a discrete system.

(b) The resulting exact nonlinear ordinary differential equations may be easily integrated using a standard Runge-Kutta

numerical integration routine. Thus, computer experiments can easily be conducted to obtain the motion of the system under consideration.

(c) The equations may be linearized about some desired reference motion and Floquet theory applied through numerical integration to investigate the stability properties. This also can be accomplished for any general configuration.

The particular results obtained by considering the lumped model are:

(1) The point mass on the end of a linear elastic massless spring is neutrally stable for the circular and elliptic orbits considered, except when the orbit has a perigee low enough to permanently alter the spin rate. Again it should be pointed out that these results and conclusions are a consequence of a numerical integration of the equations of motion and subject to computer accuracy limitations. However, no growth was detectable for a time interval of several hours and one can conclude that if an instability does exist, it must be very slowly growing.

(2) The center of mass motion may be assumed to move in a Keplerian orbit for computational purposes.

(3) For elliptic orbits, the possibility does exist that the orbit could become more circular while the relative spin rate greatly increases.

(4) Very few masses are needed to accurately predict the lowest natural frequencies of the distributed mass cable to be studied. For example, two masses will give the lowest frequency to about 4 per cent of the actual frequency.

(5) Discrete viscous dampers may be included in the analysis creating generalized forces. Results show that the axial or stretching motion

is effectively damped out, but that the transverse motion is damped only when deflections become so large as to be mathematically nonlinear: this seems to be a few percent of the length for the lowest mode.

(6) A beating phenomenon occurs between the axial motion and the transverse motion when their frequencies are close together. Large deflections can also occur when these frequencies are near each other.

(7) An additional out of orbital plane degree of freedom given to each cable mass point does not introduce an added instability into the system and, hence, can be ignored in stability considerations of systems spinning primarily in the orbital plane.

The author would like to express his great appreciation for the advice and encouragement given by Professor J. G. Eisley prior to and during the course of this investigation and to Professor F. T. Haddock and Mr. W. J. Lindsay of the Radio Astronomy Observatory, whose insight helped considerably in defining the problem area, and Professors D. T. Greenwood, R. D. Low and W. J. Anderson for reviewing and offering helpful suggestions concerning the writing of the manuscript. He would also like to thank the following members of the Radio Astronomy Observatory staff for their aid:

Mr. J. W. Greene for his many suggestions concerning the analysis and expecially his comments concerning the manuscript.

Mr. C. E. Lindahl and his computing staff for their help on the numerical analysis.

Mr. C. E. Schensted for suggestions concerning the numerical aspects of Floquet theory.

Mrs. William Klein for typing the manuscript.

REFERENCES

1. Paul, B., "Planar Librations of an Extensible Dumbbell Satellite", AIAA J., Vol. 1, 1963, pp. 411-418.

2. Pittman, D. L., Hall, B. M., "The Inherent Stability of Counter-weight Cable Connected Space Stations", Douglas Paper No. 3051, Douglas Missile and Space Systems Division, July 1964.

3. Austin, F., "Nonlinear Dynamics of a Free-Rotating Flexibly Connected Double-Mass Space Station", J. Spacecraft, Vol. 2, No. 6, November-December 1965, pp. 901-906.

4. Chobotov, V., "Gravity-Gradient Excitation of a Rotating Cable-Counter-weight Space Station in Orbit", J. Appl. Mech. December 1963, pp. 547-554.

5. Pengelly, C. D., "Preliminary Survey of Dynamic Stability of a 'Tassel Concept' Space Station", AIAA Structural Dynamics and Aeroelasticity Symposium, August 1965.

6. Tai, C. L., Loh, M. M. H., "Planar Motion of a Rotating Cable-Connected Space Station in Orbit", J. Spacecraft, Vol. 2, No. 6, November-December 1965, pp. 889-894.

7. Targoff, W., "On the Lateral Vibration of Rotating, Orbiting Cables", AIAA Paper No. 66-98, January 1966.

8. Ashley, H., "Observations on the Dynamic Behavior of Large Flexible Bodies in Orbit", AIAA J., Vol. 5, No. 3, March 1967.

9. Cesari, L., Asymptotic Behavior and Stability Problems in Ordinary Differential Equations, Academic Press Inc., New York, 1963.

10. Haddock, F. T., "Phase 1 Final Report Engineering Feasibility Study of a Kilometer Wave Orbiting Telescope", Prepared under NASA Grant NGR-23-005-131, October 1966.

11. Langhaar, H. L., Energy Methods in Applied Mechanics, John Wiley and Sons, Inc., New York, 1962.

12. Goldstein, H. Classical Mechanics, Addison-Wesley Co., Inc., Reading, Massachusetts, 1959.

13. Kaplan, W., Ordinary Differential Equations, Addison-Wesley Co., Inc., Reading, Massachusetts, 1958.

14. Pars, L. A., A Treatise on Analytical Dynamics, Heineman Educational Books Ltd., London 1965.

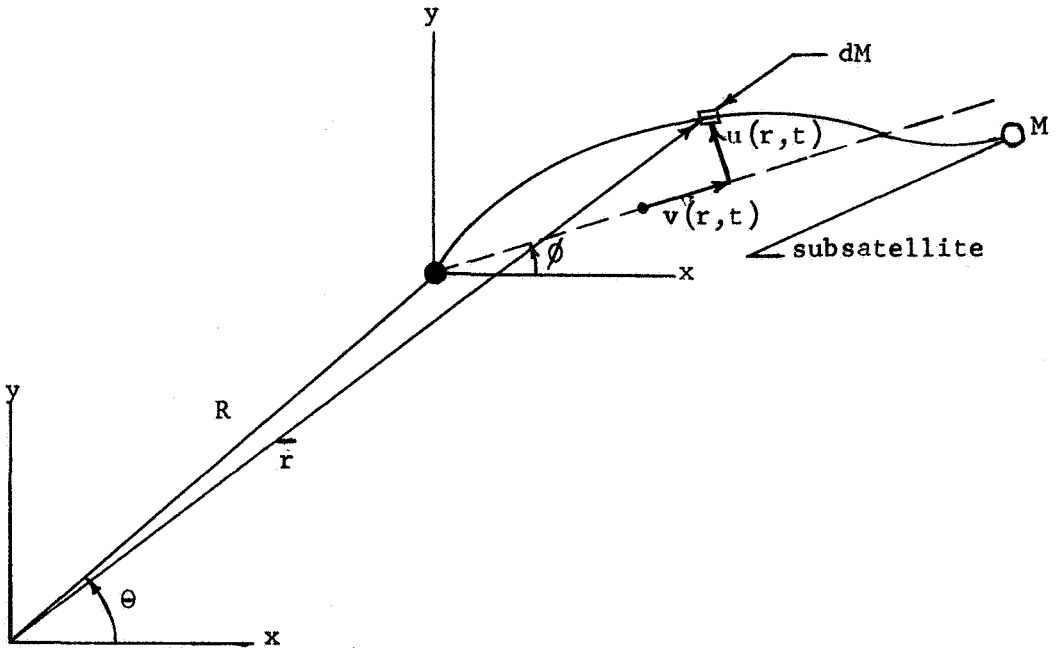

Figure 1. Coordinate system for distributed mass wire-subsatellite system

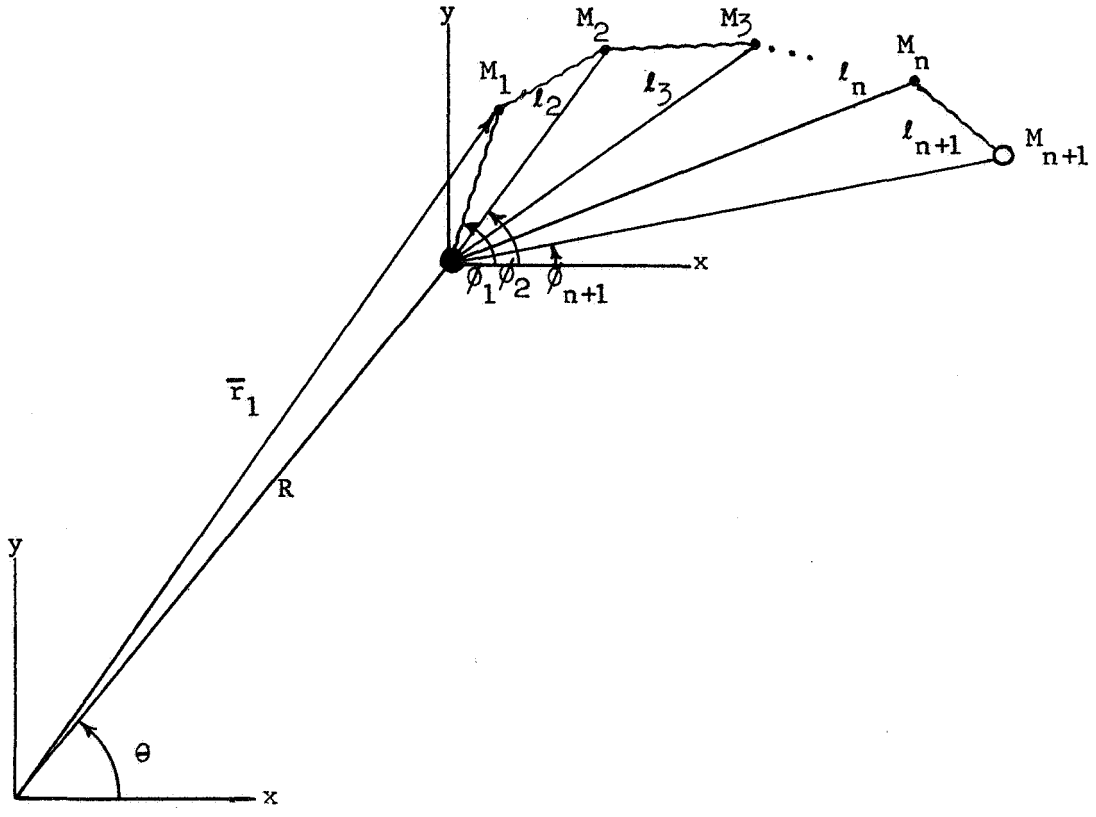

Figure 2. Coordinate system for lumped mass model

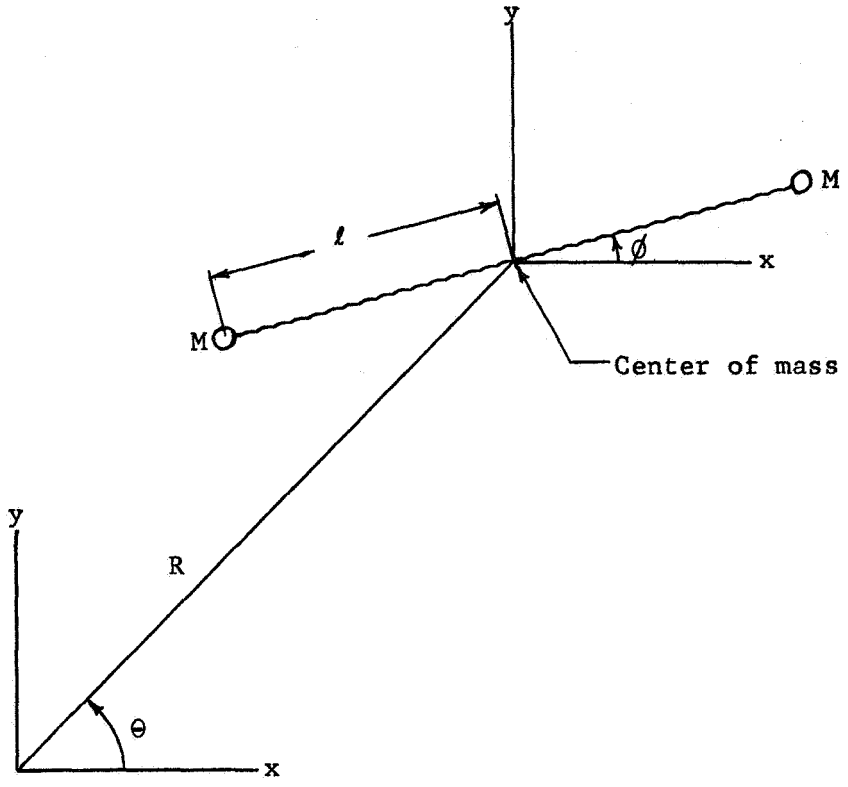

Figure 3. Dumbbell configuration

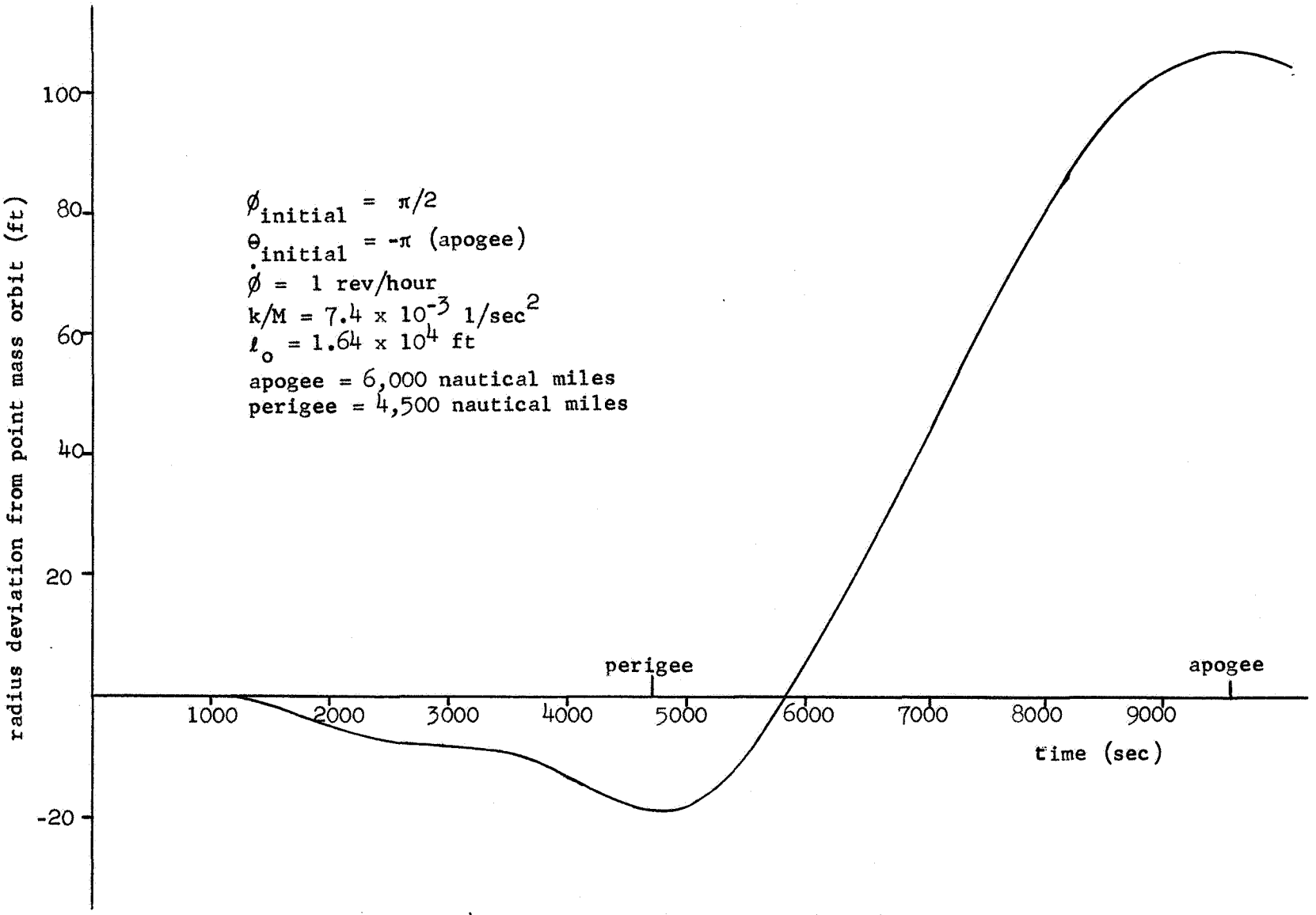

Figure 4. Deviation of orbital radial distance from that for a point mass

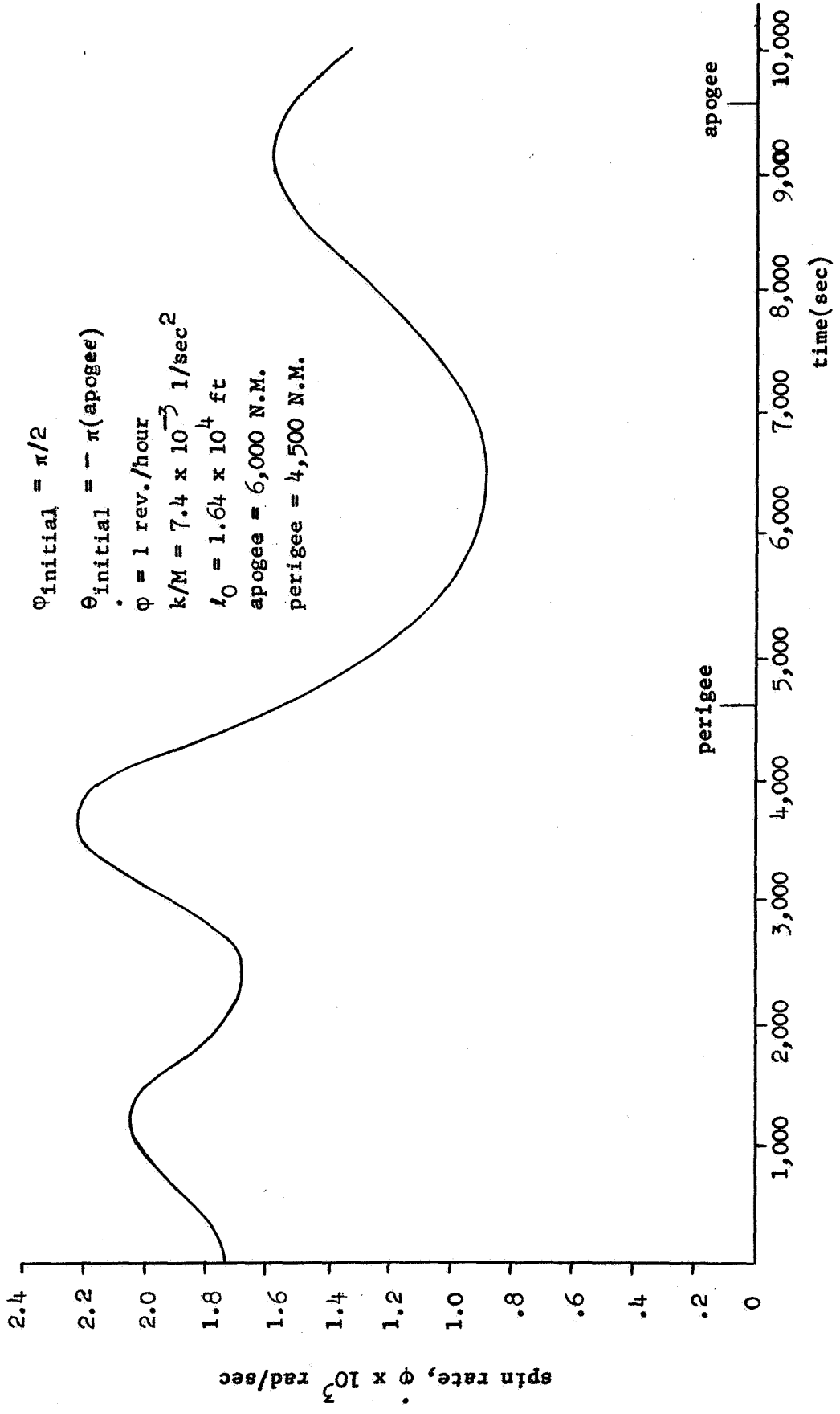

Figure 5. Deviation in spin rate

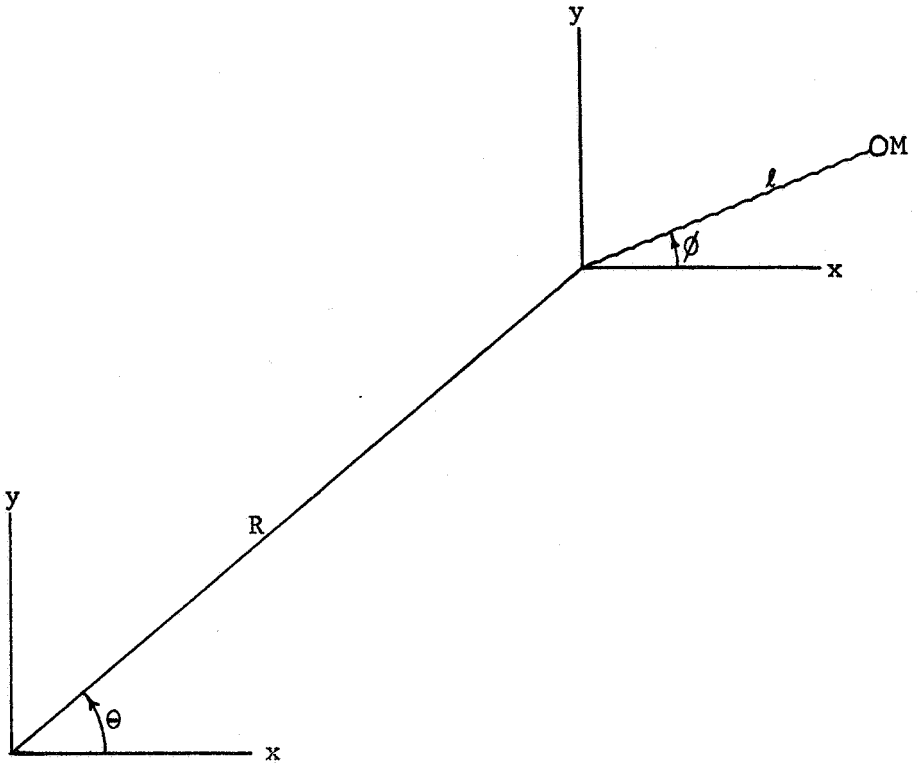

Figure 6. Single mass configuration

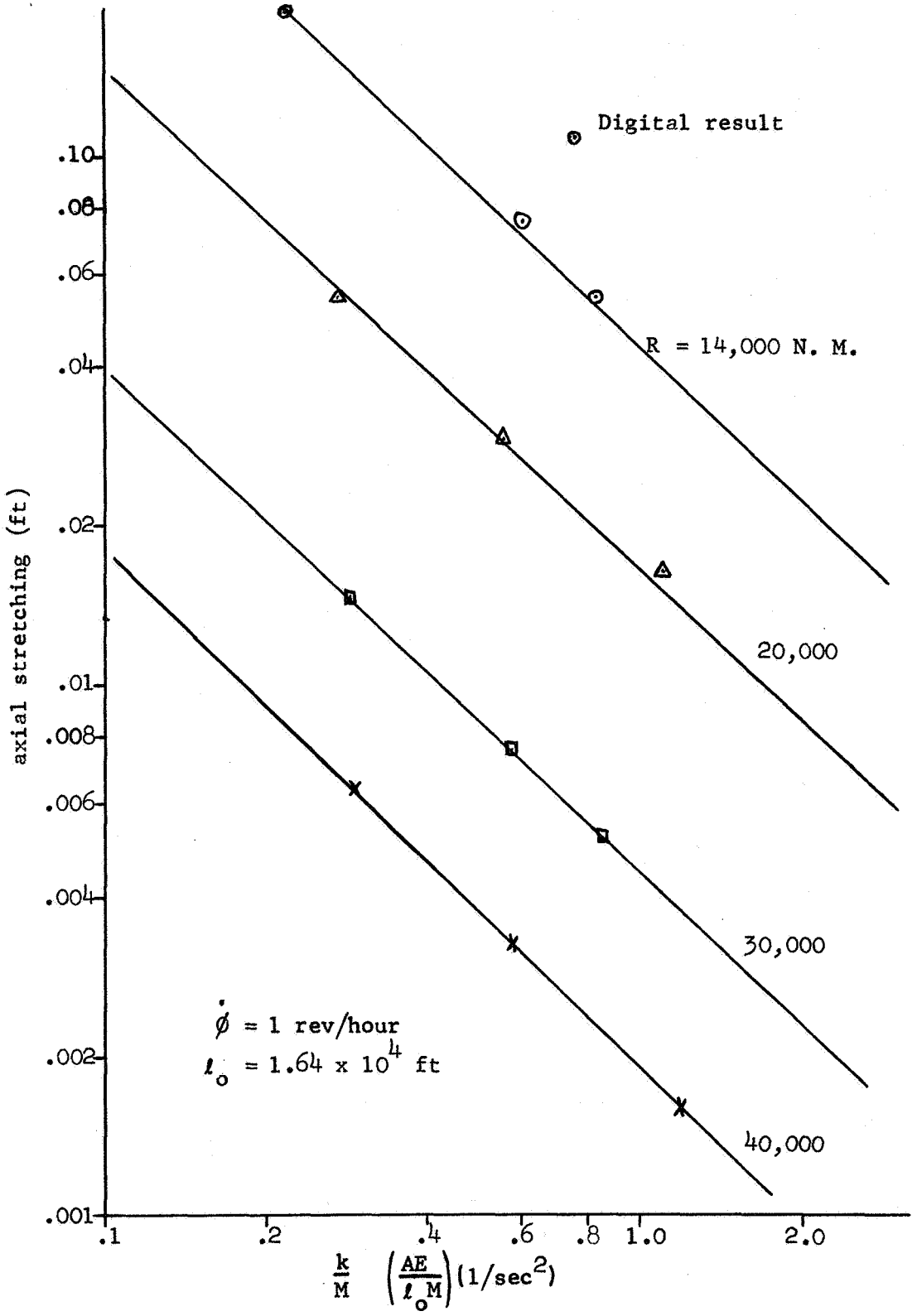

Figure 7. Axial stretching due to gravity gradient effects vs. effective spring stiffness

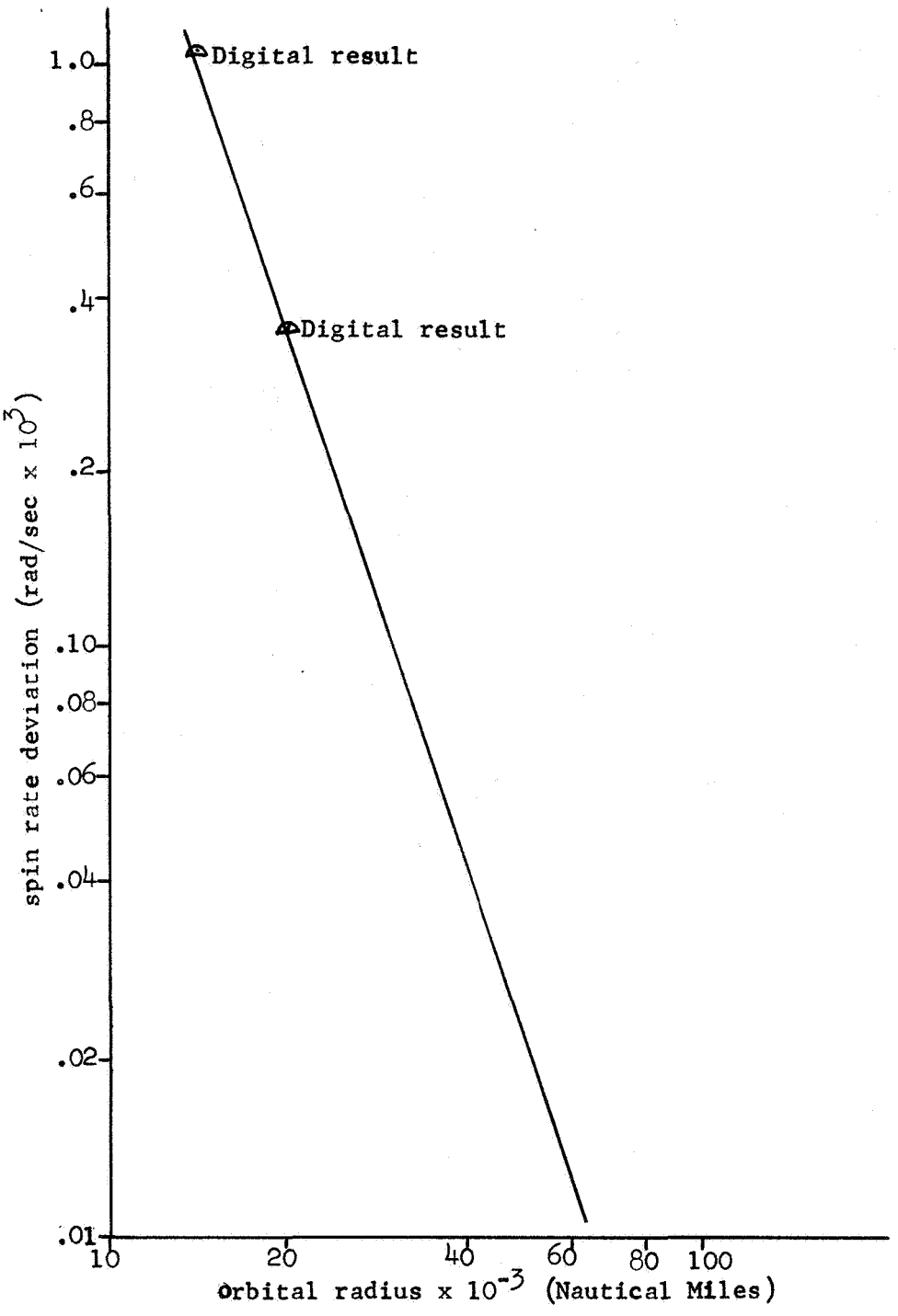

Figure 8. Spin rate deviation due to gravity gradient effects vs. orbital radius

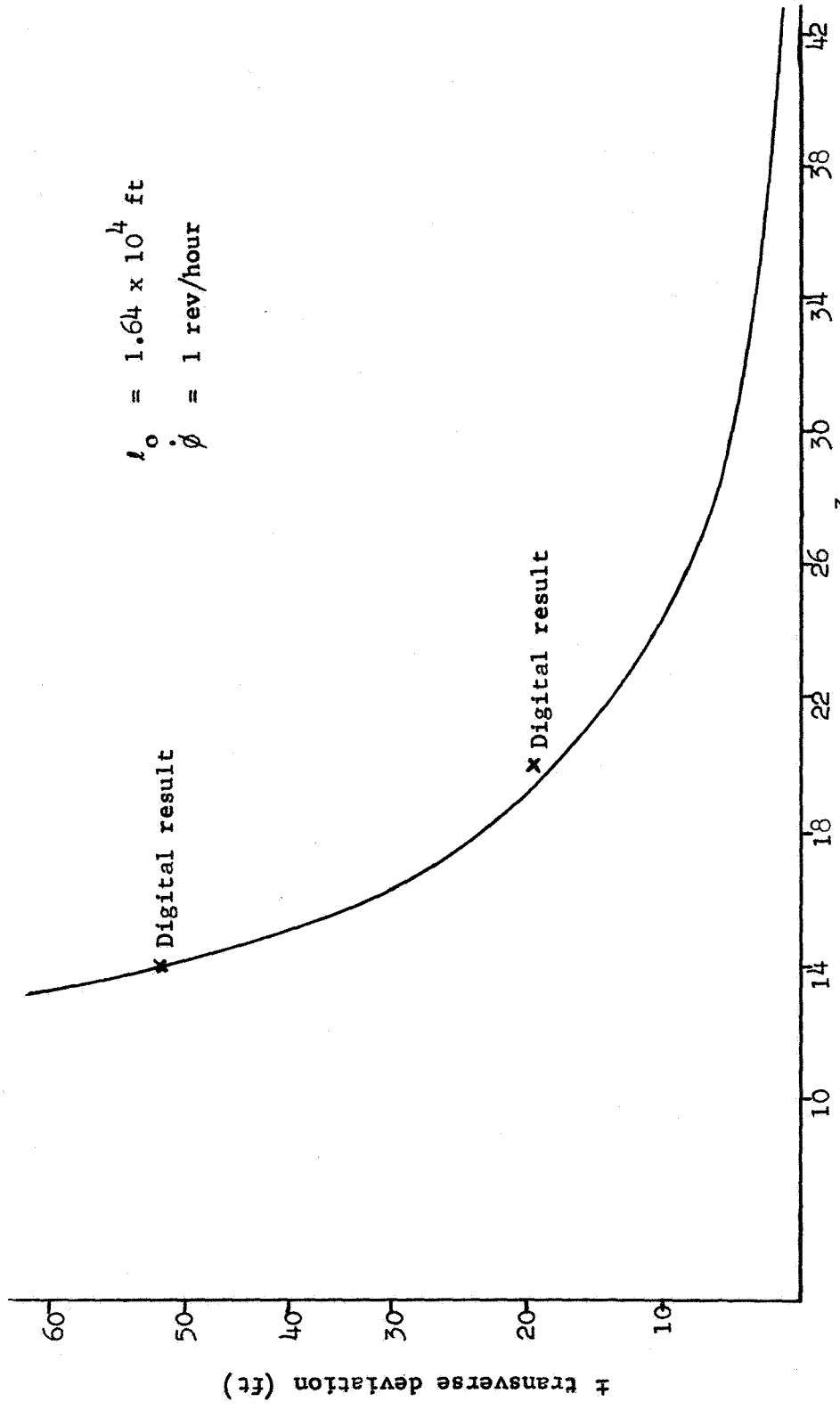

Figure 9. Transverse deviation from free space motion due to gravity gradient effects vs. orbital radius

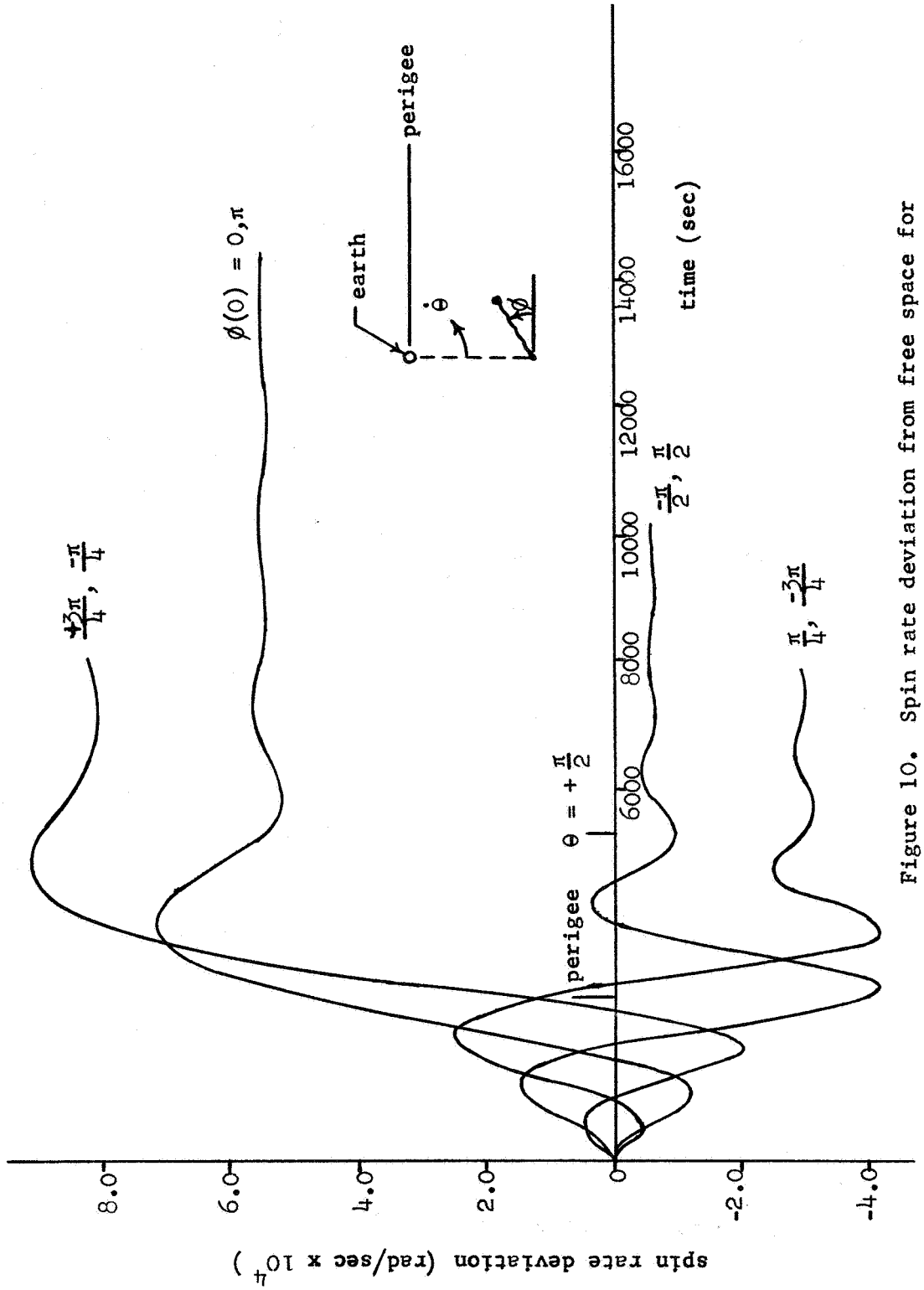

Figure 10. Spin rate deviation from free space for 60,000 by 5,000 Nautical Mile orbit

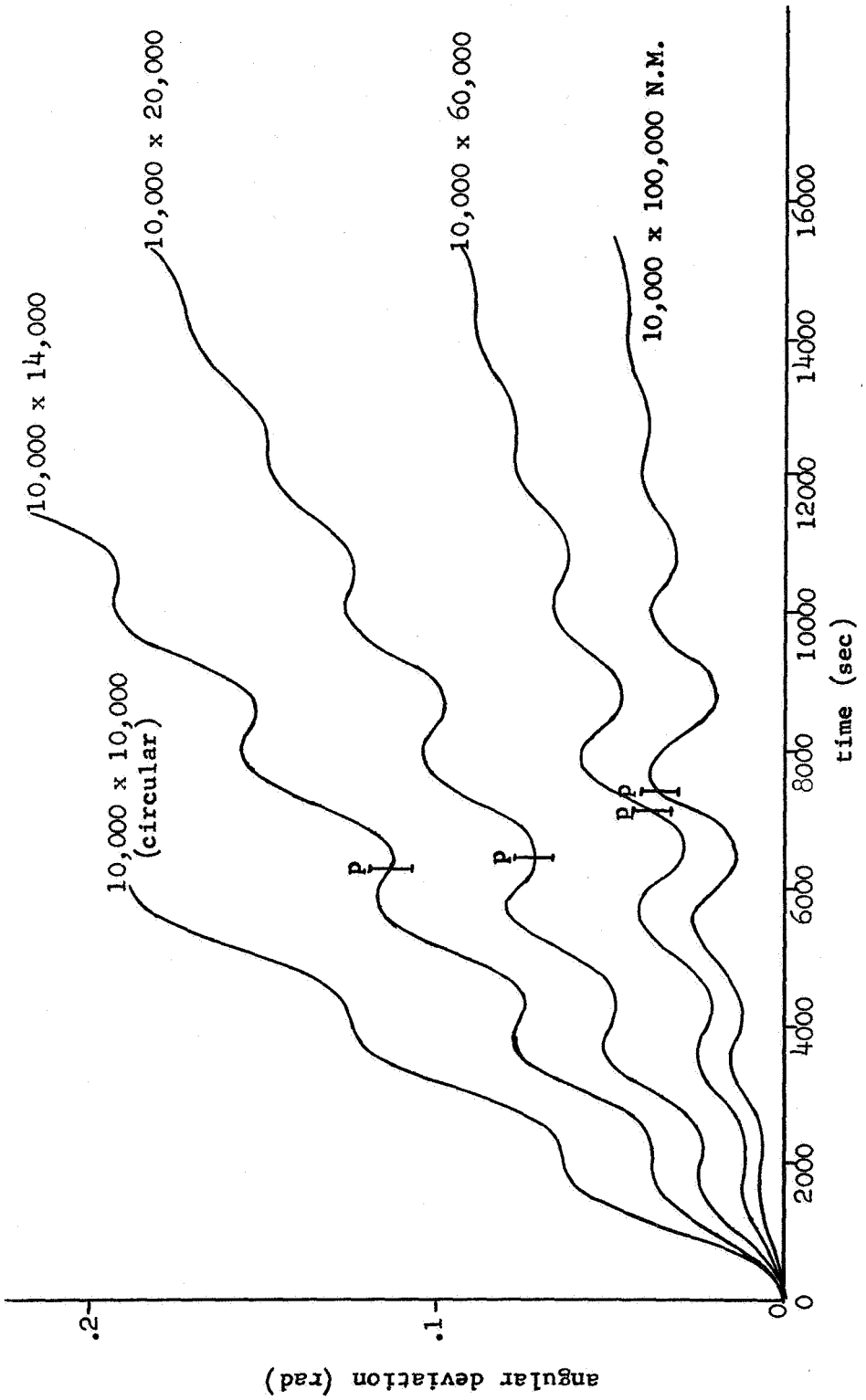

Figure 11. Angular deviation from free space for a perigee of 10,000 Nautical Miles

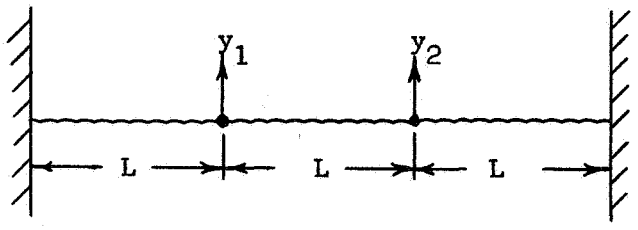

Figure 12. Non-rotating two mass configuration with fixed ends

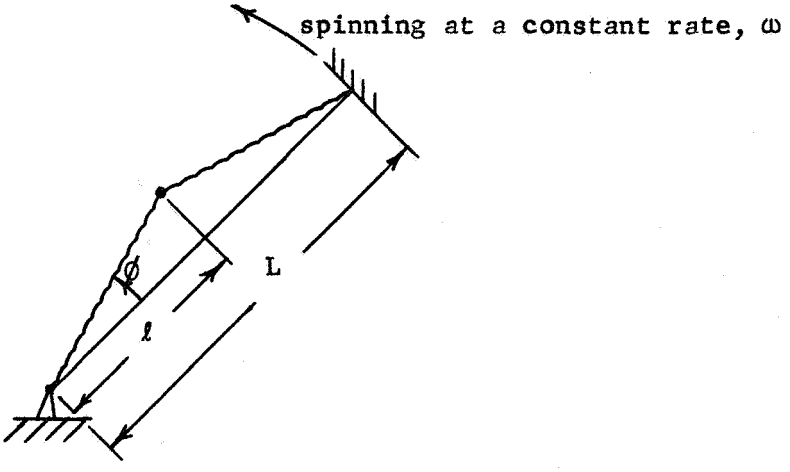

Figure 13. Rotating single mass configuration with fixed ends

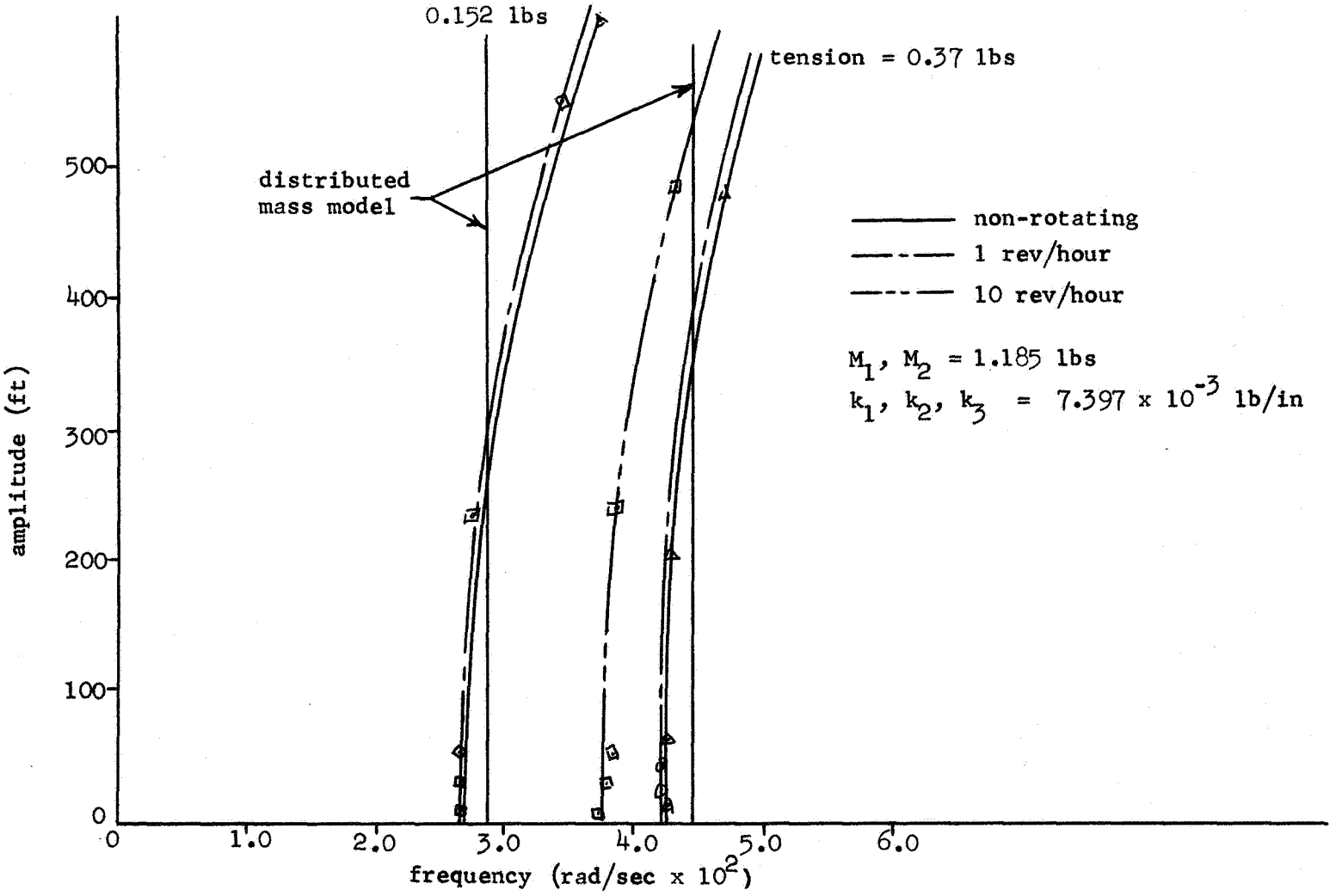

Figure 14. Transverse amplitude vs. frequency

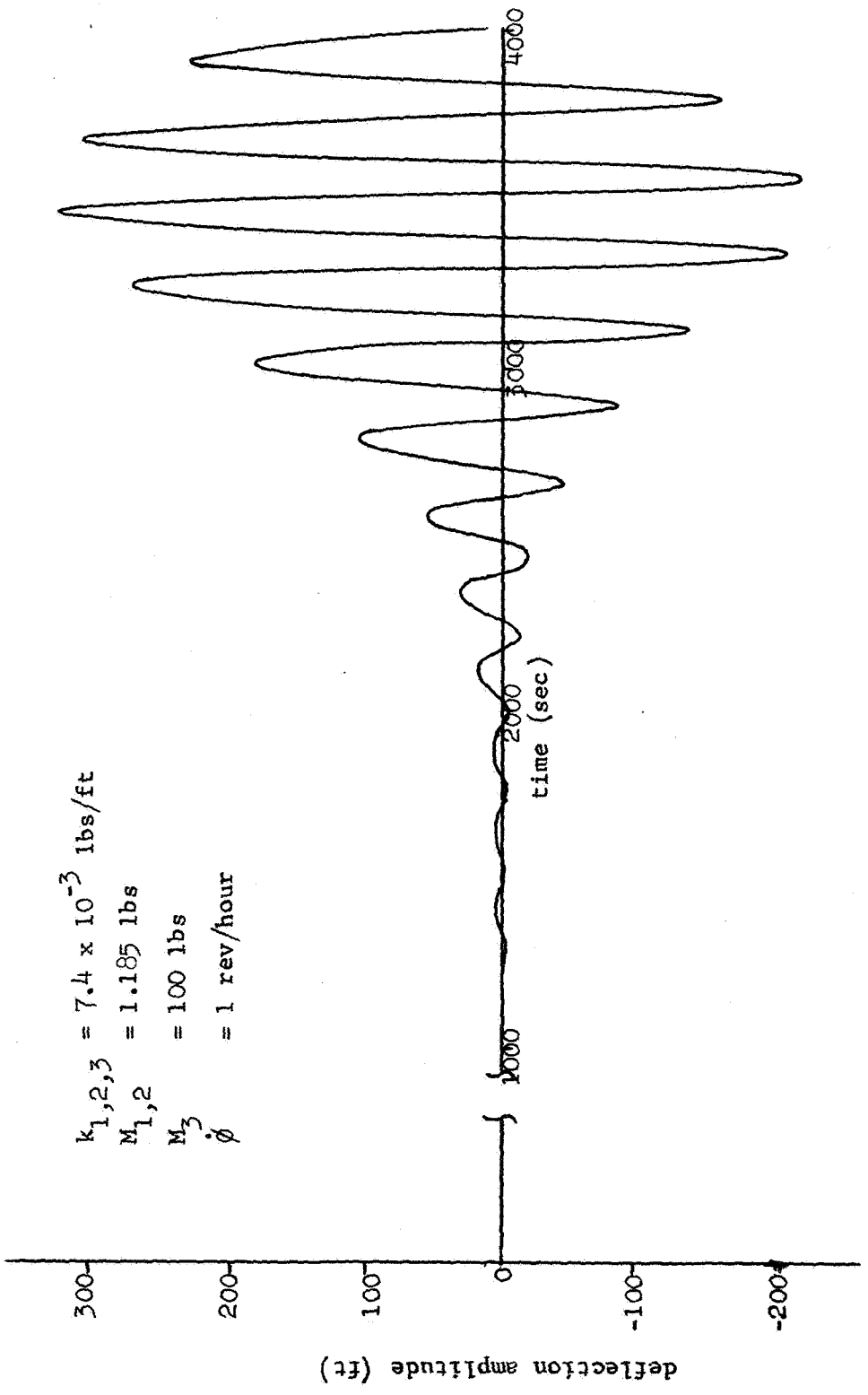

Figure 15. Transverse amplitude vs. time

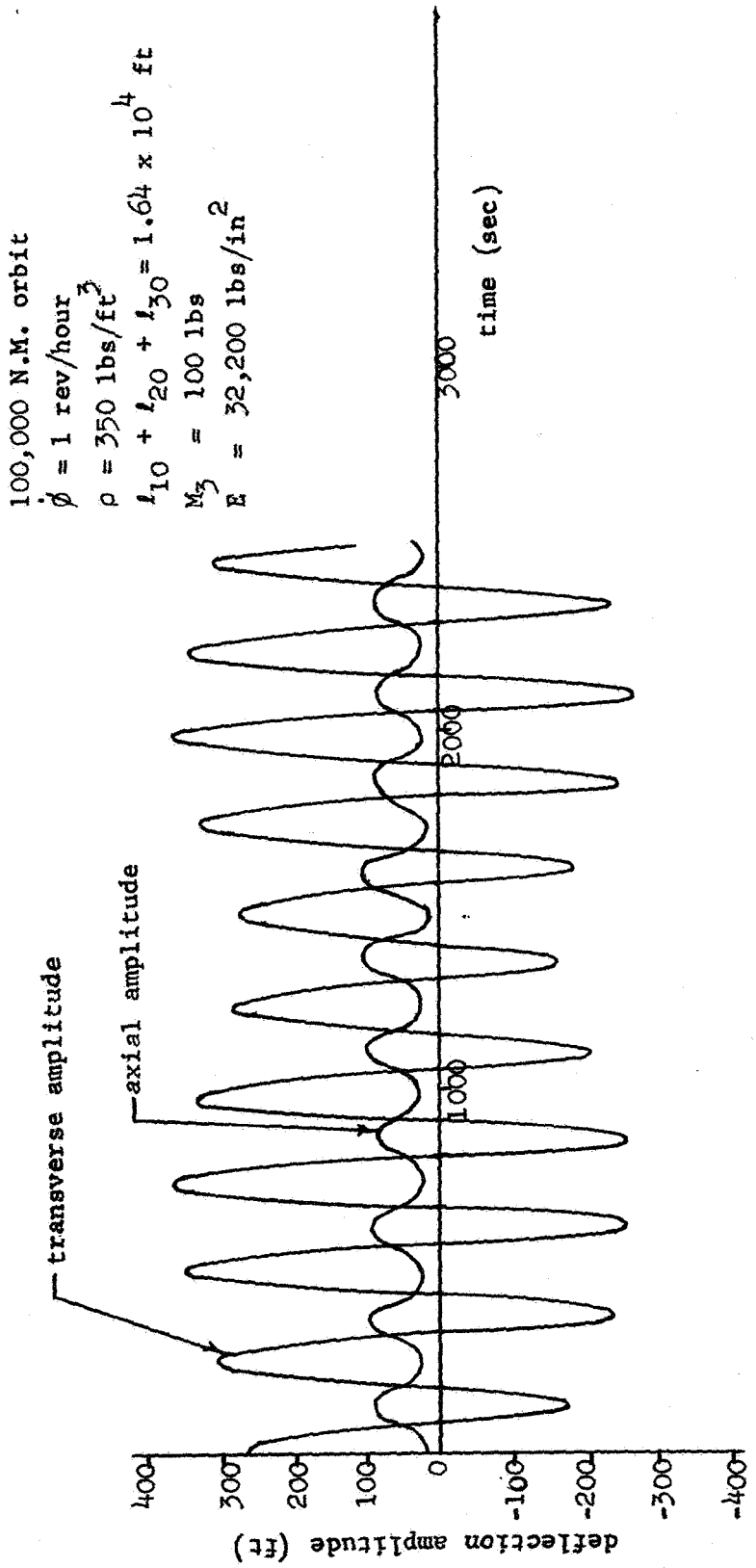

Figure 16. Transverse and axial amplitudes vs. time

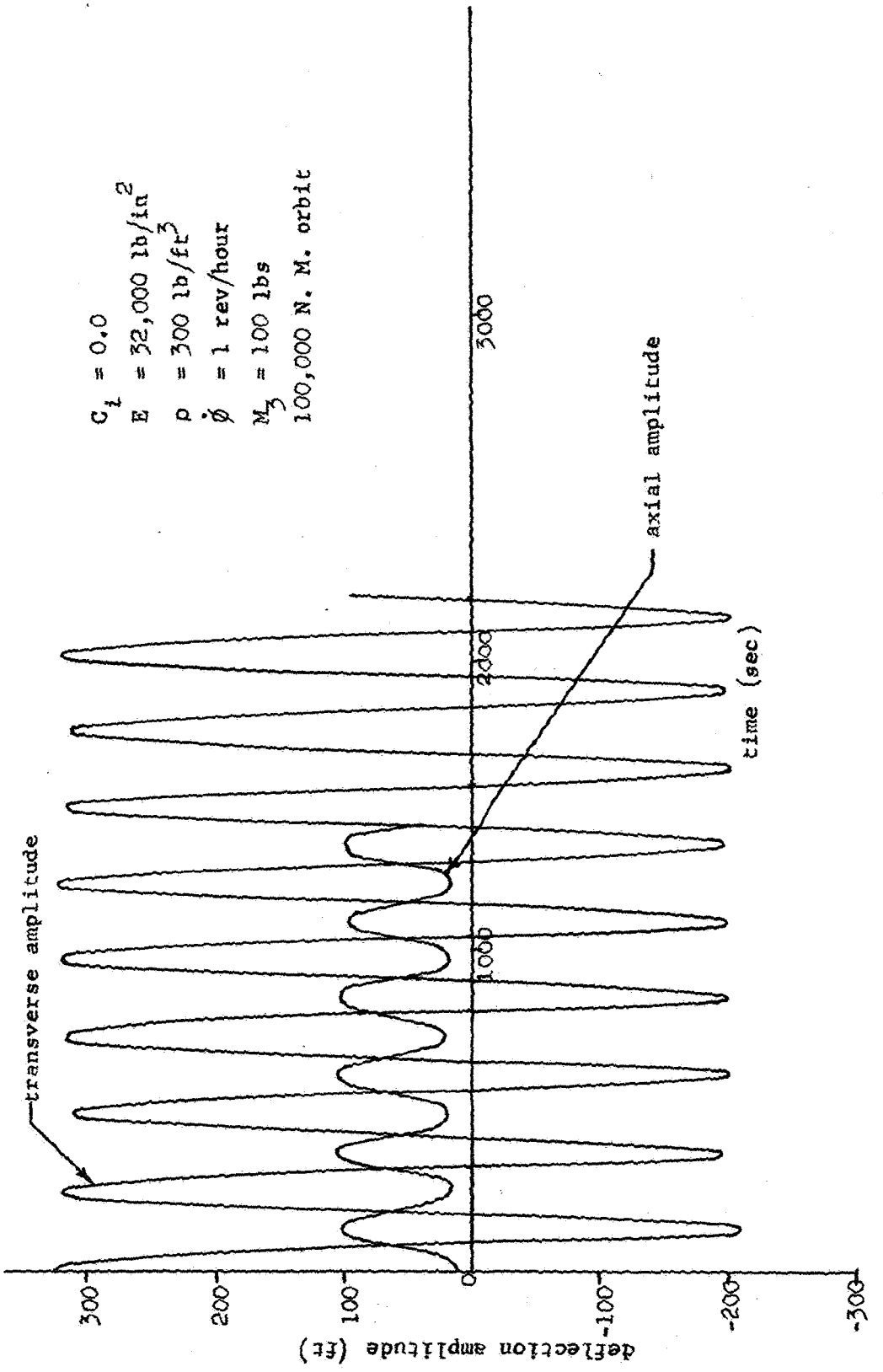

Figure 17. Transverse and axial amplitudes vs. time

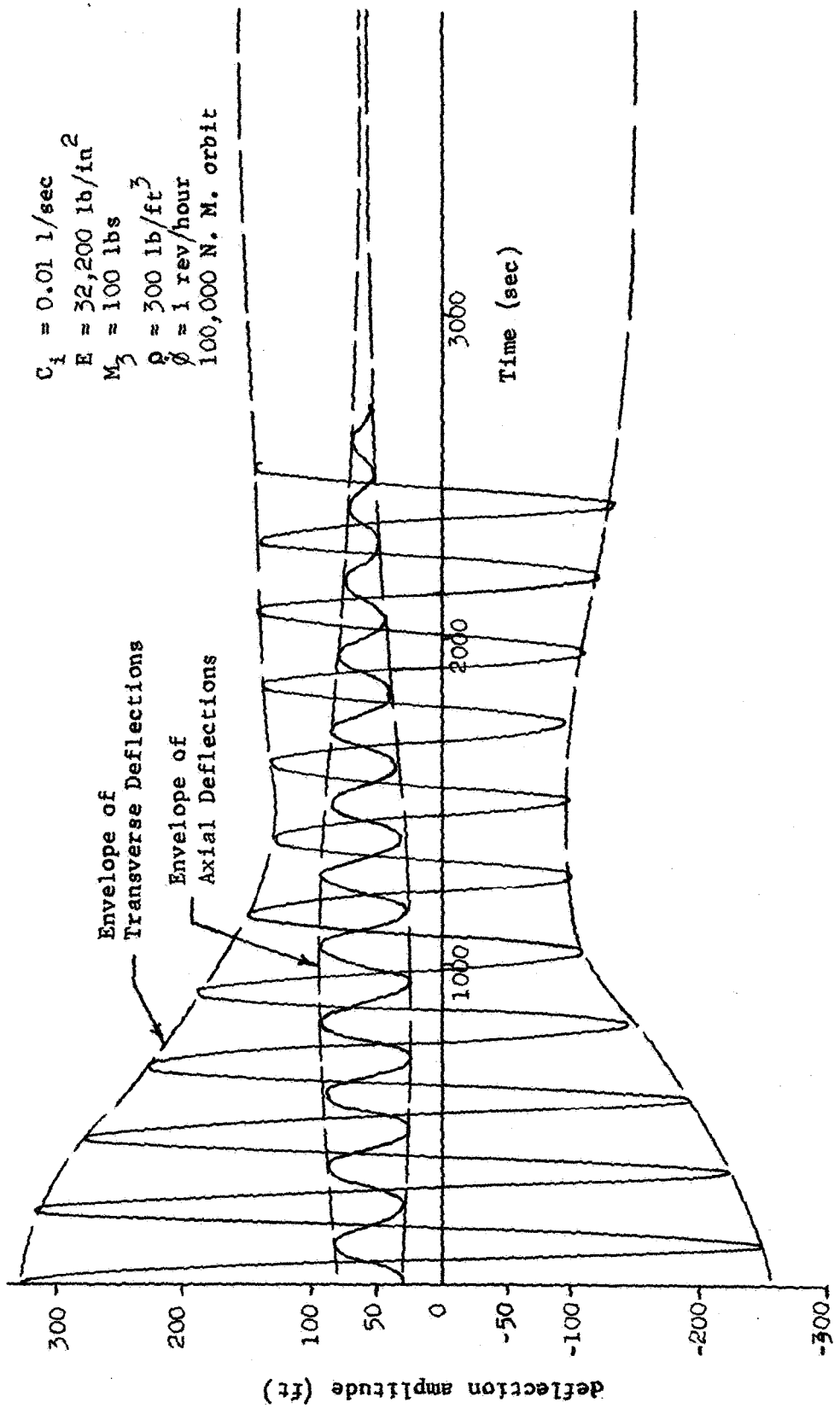

Figure 18. Transverse and axial amplitudes vs. time (damping)

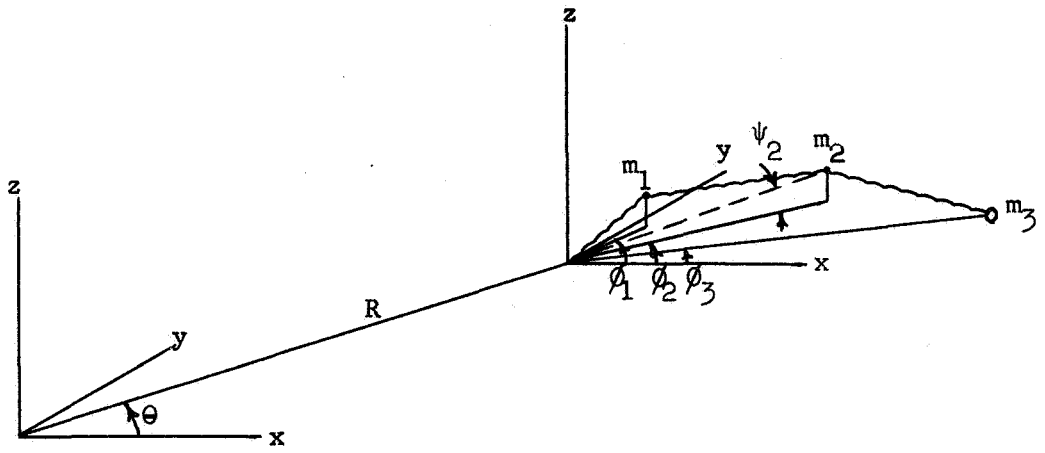

ψ_1 ≡ angle between ℓ_1 and x,y plane

ϕ_i ≡ angle between x axis and projection of ℓ_i in x,y plane

Figure 19. Coordinate system for motion out of orbital plane

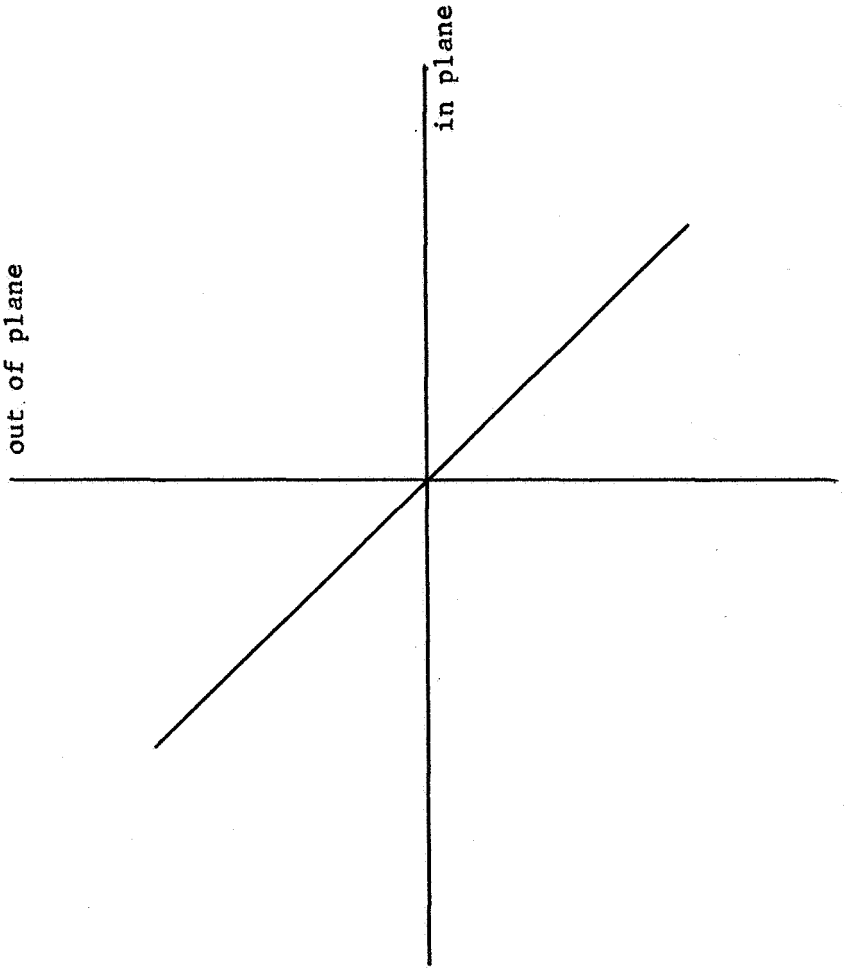

Figure 20. Out of plane amplitude (matched frequencies)

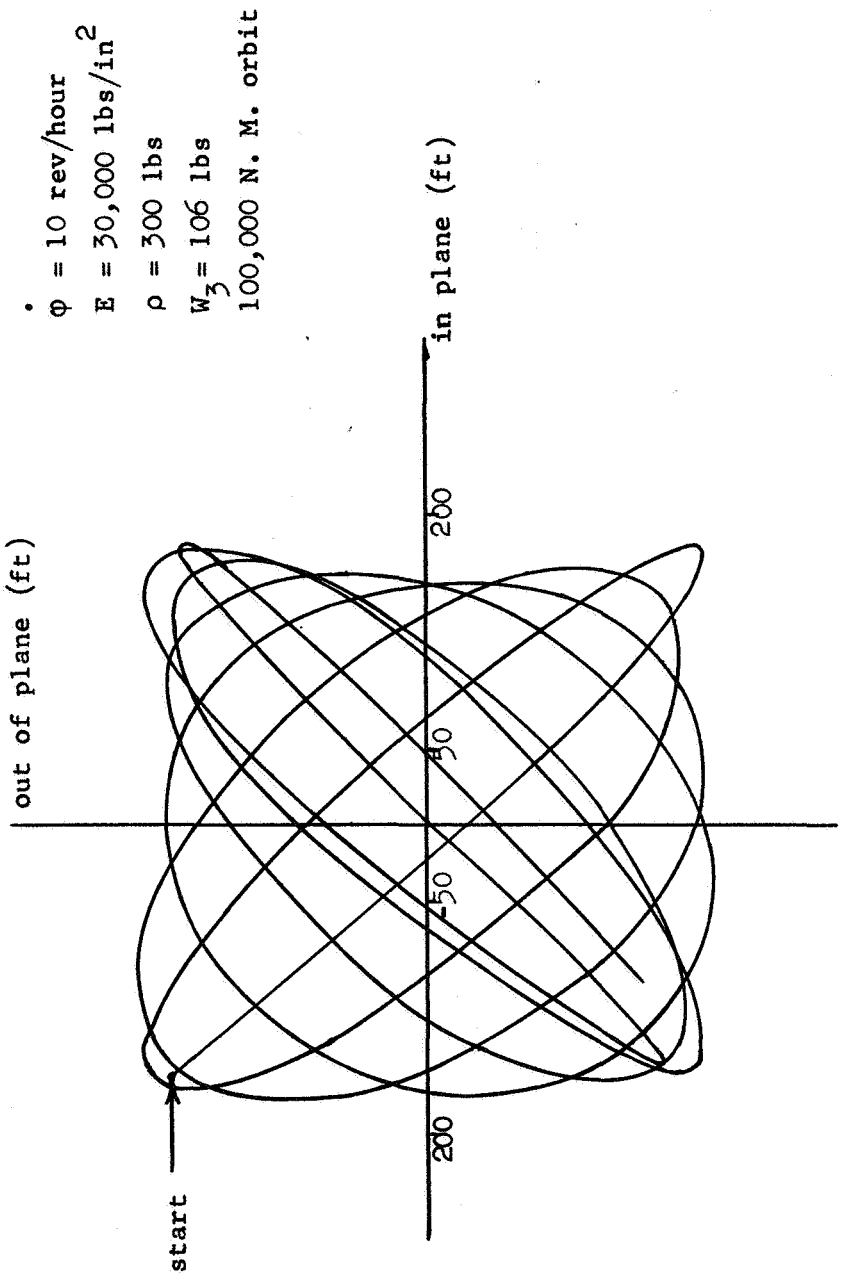

Figure 21. Out of plane amplitude (unmatched frequencies)

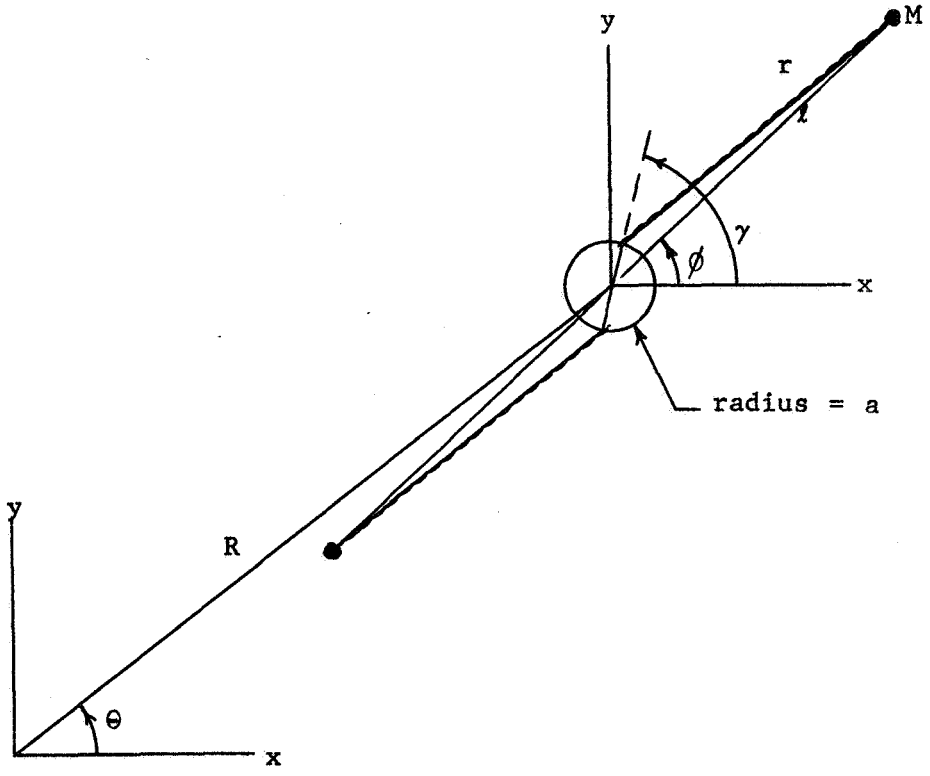

Figure 22. Coordinate system for finite central body